

5th BSME International Conference on Thermal Engineering

Techno-economic and environmental evaluation of biomass dryer

Nawshad Haque^a, Michael Somerville^a

^aCSIRO Minerals Down Under Flagship, Bag 312, Clayton South, Victoria 3168, Australia

Abstract

The pros and cons of various types of biomass dryers have been documented in this paper. Using dry biomass significantly reduces the cost of handling, transportation and pyrolysis. The main choices for drying biomass are rotary dryers, flash dryers, stationery bed dryers and fluidised bed dryers. The drying medium can be hot air, hot air mixed with steam, and/or superheated steam. A typical example for wood chip drying using a financial model is described, including the environmental performance. The energy requirements and greenhouse gas emissions have been estimated for drying biomass. From this study, it is evident that increasing temperature will decrease drying time and increase throughput but not necessarily decrease the drying cost. This is due to higher energy use and higher cost of capital inputs such as loading/unloading and heat plant. Thus, low drying temperature can be used if throughput is not a key issue for an operation. The global warming potential of the biomass drying process 9.2 kg CO₂-e/t of oven-dry biomass. This assumes that wood waste is used as fuel and drying is on a moving belt dryer. If this dry biomass is used in a power station as fuel for steam boiler, there is a significant reduction potential of CO₂ emission from a typical black coal-fired power plant due to fuel switching. This assumes that trees are planted to produce this biomass sustainably. Environmental impacts of any dryer type should be considered for selection in addition to its traditional techno-economic performance.

© 2012 The authors, Published by Elsevier Ltd. Selection and/or peer-review under responsibility of the Bangladesh Society of Mechanical Engineers

Keywords: Biomass; drying; energy footprint; greenhouse gas; carbon footprint.

1. Introduction

Biomass drying is an inevitable part of overall value chain of bioenergy. With reference to reduction of CO₂ emission, the biomass has been considered as one of the most promising future energy sources [1]. Several million tonnes of biomass such as forestry harvesting residues, wood chips, sawdust, sugarcane bagasse, and agricultural residues from grain and fruit processing [2] are available from various regions of Australia. A potentially important product from this biomass is charcoal or biochar. In metallurgical industries, particularly in iron and steel making, the application of charcoal is very promising to reduce net CO₂ emissions. Whether the product from biomass is heat, electricity, transport fuel or bio-carbon, the preparation of wet feedstock for the handling, transport, and storage are the important steps throughout this utilisation chain. This has often been ignored as the use of dry biomass is assumed in most research studies. However, biomass typically has high moisture content (i.e. 50 to 100% dry-weight basis or 0.5 to 1 kg water per kg of oven-dry biomass). The typical energy density (i.e. calorific value) of biomass doubles (e.g. from 8 MJ/kg to 20 MJ/kg for wood) with reduction in moisture content. In order to increase the energy efficiency, improve the energy quality, and reduce emissions in the energy conversion, drying of biomass to the required moisture content is important in the development of the alternative energy systems. In a boiler, the energy efficiency can be increased by 5–15% with the increased combustion temperature and by using dried instead of wet biomass and the flue gas temperature can be reduced [3]. In gasification and pyrolysis, biomass needs to be dried to 10%, to reduce the water content in the energy products, be it the charcoal or biocrude.

Although a review on biomass drying was undertaken about a decade ago [4], research into drying and processing of biomass is burgeoning [5, 6, 7]. Research into gasification of wood for combined heat and power and modelling of biomass drying research is also underway [3, 8]. There is a need for techno-economic and environmental assessment of commercial

drying and processing technology for biomass feedstock to support this research effort. In this paper, the techno-economics of drying technologies intended to prepare biomass for char making for use in iron and steel industry are assessed. Information about drying technologies for biomass (e.g. wood chips and sawdust) was collected from the open literature. A “gate to gate” life cycle assessment (LCA) results of wood chip drying have also been reported.

2. Methodology

In the open literature, information available about various dryers has been reviewed. Data collected from the literature was used to construct a financial model. This financial model has been used to assess the techno-economics of various types of dryers. In addition, theoretical energy requirements have been estimated for biomass drying with assumed specifications given here. The energy data has been used to undertake life cycle assessment of the biomass drying process. For techno-economic evaluation, the main assumptions are shown in Table 1. Drying times and thermal energy usage have been predicted from a modified drying model based on heat and mass transfer principles [9]. Thermal and electrical energy prices have been used as found from industrial sources. Labour, insurance, capital maintenance, capital insurance are assumed from standard factors as used in other CSIRO techno-economic evaluation studies [10]. All the costs are in US currency unless stated otherwise. National Greenhouse Accounts (NGA) factors and methods have been used to estimate CO₂ equivalent emission [11].

Table 1: Main assumptions for techno-economic evaluation

Inputs	Values	Unit
Wood species	Radiata pine (<i>Pinus radiata</i>)	Unit
Woody biomass particle size	5	mm
Initial moisture content (oven-dry basis)	50	%
Final moisture content (oven-dry basis)	10	%
Air-flow around the material	0.2	m/s
Relative humidity	5	%
Drying temperature	50-200	°C
Dryer type	Conventional hot-air based industrial dryer	
Estimated dryer total cost including installation	6,600,000	US\$ (Y 2010)

The main selected environmental impact categories for earlier LCA studies at CSIRO were gross energy requirement (GER) which is used to estimate global warming potential (GWP) or greenhouse gas emissions expressed as CO₂ equivalent or CO₂-e [12]. GWP was calculated and reported based on this estimated GER.

3. Results and Discussion

3.1. General Features of the Drying Process

Some distinguishing features of the drying unit operation are the variation in the material size and shape, variety of drying media used and the large range of drying times [13]. This is why, there are over 400 different types of dryers reported in the literature and over 100 distinct types of dryers are commonly available. The essential mechanisms involved with biomass drying are diffusion of bound moisture and bulk water mass transfer which depends on the applied temperature. The water vapour is carried away by forced or natural air flow in the dryer. Drying is a coupled heat and mass transfer process. This can either be enhanced or decreased depending the conditions employed surrounding the material to be dried. However, the radiant and conduction heat from the dryer wall can be significant in some situations. The selection of a dryer is rather complex since several choices can exist and the final decision depends on numerous criteria. It is also better to focus on the whole drying system (heating system, any pre or post-drying processes or treatment) rather than just the dryer itself. Computer-aided decision making software systems have been developed (e.g. DrySel software by ASPEN Tech Process Tools [14]) to choose appropriate dryers for a variety of products. However, product and feed-material specific dryer selection still needs some sound judgments. The main three requirements of a dryer are that the supply of heat (either with hot air or in mixture with steam), a carrier to remove the water evaporated from the material during drying, and the exposure of the wet surface to the drying medium by agitation or other means.

3.2. Dryers for Biomass

There are several dryers currently available for biomass. These are grouped in various categories based on the handling of particles in terms of size, uniformity, the mode of heating, and the capital and operating costs. The biomass particle can be heterogeneous in terms of weight, shape and density. Forestry residues are a mixture of woody and foliage components of trees with a variety of shapes, sizes, density and complexity in nature for handling and processing. The first step can be the size reduction and sorting in at least three bins based on the density and shape.

3.3. Description of Dryers

The descriptions of fluidised bed drying, rotary drum, flash dryer, fixed bed, solar and ambient air drying are given below. Textbooks cover many general aspects of fluidised bed drying [15]. Proper fluidised bed drying occurs after fluidising in dense fluid rather than in dilute fluid (which occurs with pneumatic flash drying). The important considerations are bed height and the velocity of air (e.g. operating superficial) at the chosen temperature as this dictates energy requirement. Fluidised bed drying can be batch or in continuous mode. Additional key variables are flow of the materials ($\text{kg/m}^2\text{h}$) and hold up (kg/m^2) in the furnace.

Rotary drum dryers are a common dryer type for larger woody biomass material such as wood chip for making particle board. The dryer consists of a cylindrical shell, inclined at a small degree to the horizontal (10-30% slope or 0.1 to 0.2 m/m) and rotating at about 1 to 10 rpm. The flue gas or hot gas is directly supplied to the drum which is rotated mechanically by an electric motor. The general temperature employed is around 200°C but should not be above 250°C .

Flash drying is also called fluidising and drying in dilute fluid. The finer particles are flown through a very long steel tube (more than 100 m in length and 0.3 to 0.5 m in diameter). Drying load for high capacity modern dryers should be at least 20 tonnes of water evaporated per hour [16]. A stream of very hot air at high flow velocity (over 16 m/s) is passed through the tube. The air sucks the particles and exposes particles to the drying medium. This is usually done in a single or two stages. The typical residence time for each particle is only a few seconds (3-5 s) in the tube.

Bed drying is a biomass layer that is supported on a perforated belt which can either be stationary base or on a moving belt. Hot air is passed through the bed. The particles do not fluidise and thus do not require higher air flows. The depth of bed is generally recommended to be 0.4 to 0.6 m. Experimental drying tests reported [7] that the drying time would be around five hours for sawdust and ten hours for wood chips in fixed bed drying with moderate temperature (from 40 to 70°C) and low air velocity (0.2 to 1 m/s). The Bruks Klockner Wood Technology (equipment manufacturing company) based in Germany has released a commercial unit of bed dryer for sawdust, bark and woodchip [17]. The operating temperature is 80 - 110°C over the bed. An infeed auger spreads the material evenly across the dryer's entire width. The hot air passes through the slowly advancing moving bed from below through the perforated bottom plates. The moist air is discharged outside by axial fans. The required estimated thermal power for a unit with 75 m^2 bed area is about 2.6 MW. The average outfeed capacity for such a unit is 2 tonnes dry product per hour if the moisture content is reduced from an initial 60% to 10% (wet-basis).

Over the last few decades, much research and development has been conducted into the use of solar drying [18]. Large rectangular trays with coarse mesh or perforated plate can be used for biomass drying with some other necessary modifications of the solar timber kiln.

Drying under the shed (barn drying) or in the open sun (in a heap) is common ambient air drying using atmospheric heat. The ground should be made level, preferably with an impervious lining or concrete paving with slight slope and with a good exposure to passing wind and good drainage. The heap needs to be mixed up together every now and then.

3.4. Techno-Economic Evaluation of Biomass Drying

Drying times and thermal energy consumption were estimated using biomass drying models based on original wood drying models [9]. Figure 1 shows typical drying time and corresponding thermal energy requirement for a tonne of dry product at various temperatures. Figure 2 shows the throughput increase for an increase in temperature and resulting operating cost. The drying time is inversely proportional to temperature as expected provided other assumptions remain same. However, the estimated theoretical thermal energy requirement is expected to increase with higher drying temperature as shown in Figure 1. Since the drying time is expected to reduce, throughput will increase as shown in Figure 2.

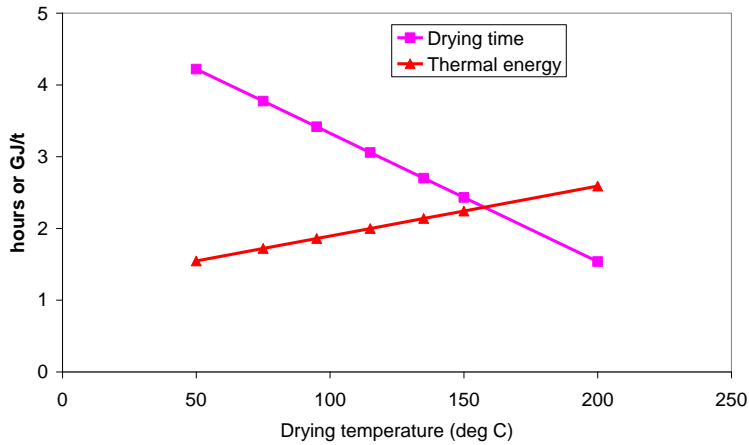


Fig. 1: Drying time and gross thermal energy requirement as function drying temperature.

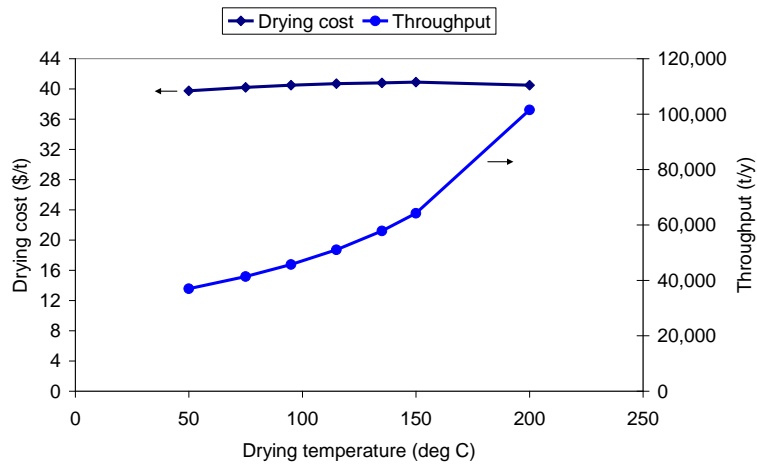


Fig. 2: Throughput and drying cost as a function drying temperature.

Although the throughput increase should decrease the cost per unit dry product, this is not straightforward for two main reasons. Firstly, increasing throughput will require increase in the capital items due to handling and processing of more materials. The capital cost for a new throughput can be estimated using equations found in the literature [19]. A power law equation (Eq 1) is commonly used to scale plant and equipment costs with changes in throughput or capacity.

$$\text{New plant cost} = (\text{New capacity}/\text{base capacity})^{0.65} \text{ (Eq 1)}$$

An exponent value of 0.60 – 0.65 is widely used for this purpose for most equipment [19]. Thus with the increase in throughput within a certain range, the capital cost is expected to increase with its maintenance and depreciation. This capital includes dryers and necessary feeding/unloading infrastructure including heat generation system (i.e. heat plant). Secondly, increasing temperature is associated with increase in energy consumption. Thus, the operating utility cost (i.e. for thermal energy) is expected to increase. However, since more materials are processed, there is no significant overall increase in drying costs. From this assessment, it is evident that increasing temperature will decrease drying time and increase throughput but not necessarily the drying cost. The operating cost was predicted to be around \$40/t dry product from the financial model used in this paper.

A company based in Germany called Barr-Rosin under the Gesellschaft für Entstaubungsanlagen (GEA) Group of Companies has developed a commercial drying system for biomass such as sawdust and wood chips using superheated steam. The capital cost of this dryer unit is AU\$15 M for a 20 tonne/h evaporation load reported in Barr-Rosin brochure 2009 [17]. The operating cost in Europe was estimated to be around AU\$31/tonne of water evaporated. Independent calculations for this paper from the re-constructed financial model based on Barr-Rosin data found the operating cost was AU\$35/t dry product or AU\$54/t water evaporated. In terms of cheaper drying, ambient air and solar drying can be considered where throughput, control and dry product quality requirements are not so stringent. The likely cost of solar drying would be around AU\$15/tonne of wet biomass as was quoted by an equipment supplier. This translates to about

AU\$47/tonne of water evaporated (2010). Typical high temperature wood drying cost is around AU\$50/t of wood (industry visit).

3.5. Energy and CO₂ Emission from Biomass Drying

Drying thermal energy has been calculated based on 1.64 GJ/t of water removed from biomass at 95°C, as predicted by the drying model. About 0.68 t of water needs to be removed to produce a tonne of oven-dry biomass, if the initial moisture content is 68% (dry-basis). The thermal energy requirement was calculated to be 1.12 GJ/t oven-dry biomass. Drying thermal energy is assumed to be sourced from burning woody waste with 85% boiler efficiency. For obtaining 1.32 GJ thermal energy, 81 kg of wood waste is used as fuel. Wood has specific energy of 16.2 GJ/t. The emission factor for wood combustion is calculated to be 20.7 kg CO₂-e/t dry wood [11]. Thus emission from drying thermal energy using waste wood as a fuel is 1.69 kg CO₂-e/t of oven-dry biomass. Similarly, the factors can be estimated based on other fuels used for energy in drying.

Dryer electrical energy has been estimated based on the assumption that two motors at 10 kW power are required for a rotary drum dryer with 4 t/h drying capacity (industry visit). The electrical energy is calculated to be 5 kWh/t of raw biomass. This is equal to 4.5 kg CO₂-e/t of biomass with black-coal based electricity emission factor. According to NGA factor, black-coal based electricity has 0.9 kg CO₂-e/kWh electricity. This is equal to 7.6 kg CO₂-e/t oven-dry biomass since 1.68 tonnes of biomass are processed to produce 1 tonne oven-dry biomass. Thus total CO₂ emission from drying using both thermal and electrical energy is 9.3 kg/t of oven-dry biomass. The specific GHG emission for dry product can be used to estimate the GHG emission per year of a typical drying plant. The GHG footprint of a typical drying plant with 500,000 t/y capacity can vary for various fuel types. The estimated emission from the dryer is 4,643 t CO₂-e/year for wood-waste based fuel. These emissions are 4,788 t for bagasse, 7226 t for charcoal, 36,617 t for natural gas and 62,060 t CO₂-e/y for black coal based fuel source.

A hypothetical scenario can be assessed here. If this plant produces dry wood chip for electrical power generation, there is a potential reduction of CO₂ emission from a power plant compared with a coal-fired power plant of the same capacity. This is based on the assumption that wood is produced sustainably using plantation rotation in perpetuity. The above mentioned drying plant can supply dry fuel for a 80 MWe power plant per year. The CO₂ emission reduction potential is highest if biomass based fuel is used rather fossil carbon such as black coal for the source of thermal energy for the dryer. This assessment shows that there is a potential emission reduction of about 0.6 Mt of CO₂ compared with that from a typical coal-fired power plant of this size. With the introduction of carbon tax, this is about AU\$13.8 M tax savings for the power plant assuming a \$23/t CO₂-e. The carbon footprint for biomass drying is 0.8% of the total emission from this power plant. If this dry wood is used for this power station, there is a significant reduction potential of CO₂ emission from this black coal-fired power plant.

3.6. Other Environmental Aspects of Biomass Drying

The main issues in biomass drying would be energy efficiency, environmental impacts, risk of fire, and costs. Because biomass is combustible, with an auto-ignition temperature of 260–288°C, the risk of fire needs particular attention. The environmental impact with biomass drying is another issue that needs to be considered carefully. The emission of resins and other organic acids can cause ‘‘blue haze’’, a common phenomenon due to the condensation of the chemical components of biomass. Unregulated and uncontrolled emissions of nitrogen oxide (NO_x), formaldehyde (HCHO), and particulate matters can also damage the local environment. Generally drying temperature for woody biomass is recommended below 150°C to avoid emission of the wood chemical components. Short drying period of up to 200°C can be considered, however, above 250°C wood chemical components will breakdown, degrade and will be likely to emit blue haze.

4. Conclusions

Using dry biomass to produce energy for dryers has significant advantages as the handling, transportation and pyrolysis process reduces the cost. Three main choices for drying biomass are rotary dryers, flash dryers and fluidised bed dryers. The drying medium can be pure hot air, hot air with steam, and pure superheated steam. From this study, it is evident that increasing temperature will decrease drying time and increase throughput but not necessarily decrease the drying cost due to higher energy use and part of capital inputs such as loading/unloading and heat plant. Thus low drying temperature can be used if throughput is not a key issue for an operation. The total global warming potential of biomass drying process as expressed in CO₂ equivalent units is 9.3 kg/t of oven-dry biomass using dry wood waste as fuel for a rotary drum dryer. If this dry wood is used for a power station, there is a significant reduction potential of CO₂ emission compared with that from

a typical black coal-fired power plant. This assumes that trees are planted to produce this biomass sustainably. Environmental impacts of any dryer type should be considered for selection. This is to determine energy requirement and efficiency and the net gain of energy in the biomass after drying. The other important factor is the temperatures, since at much higher temperature (above 300°C) the emissions to the air are likely to be under scrutiny by the regulatory authorities.

Acknowledgements

This work was carried out under the auspice and financial support of the CSIRO Minerals Down Under Flagship Research Program.

References

- [1] Rentstorm, R. The potentials of improvements in the energy systems of sawmills when coupled dryers are used for drying of wood fuels and wood products. *Biomass and Bioenergy* 2006;30: 452-460.
- [2] Haque, N, Somerville, M, Jahanshahi, S, Mathieson, JG, Ridgeway, P. Survey of sustainable biomass for the iron and steel industry. Proceedings of the CSRP Conference 2008, Brisbane 17-19 November, 2008.
- [3] Pang, S. Guest Editorial Biomass Drying: Areas for future R&D needs and sustainable energy development. *Drying Technology* 2008;26:623–624.
- [4] Brammer, JG, Bridgwater, AV. Drying technologies for an integrated gasification bio-energy plant. *Renewable and Sustainable Energy Reviews* 1999; 3:243-289.
- [5] Bridgwater, AV. Renewable fuels and chemicals by thermal processing of biomass. *Chemical Engineering Journal* 2003; 91:87–102.
- [6] Reyes, A, Vega, R, Garcí'a, G. Drying sawdust in a pulsed fluidized bed. *Drying Technology* 2008;26: 476–486.
- [7] Bengtsson, P. Experimental analysis of low-temperature bed drying of wooden biomass particles. *Drying Technology* 2008;26:602–610.
- [8] Pang, S., Mujumdar, AS Drying of woody biomass for bioenergy: Drying technologies and optimisation for an Integrated Bioenergy Plant. *Drying Technology* 2010;28:690-701.
- [9] Haque, MN . Simulation of temperature and moisture content profiles in a *Pinus radiata* board during high-temperature drying. *Drying Technology – An International Journal* 2007; 25(4):547-555.
- [10] Bruckard, WJ, Davey, KJ, Jorgensen, FRA, Wright, S, Brew, D, Haque, N, Vance, ER. Development of an integrated early removal process for the beneficiation of arsenic-bearing copper ores. *Minerals Engineering* 2010; 23(15):1167-1173.
- [11] Commonwealth of Australia. National Greenhouse Accounts (NGA) Factor. Department of Climate Change and Energy Efficiency, Canberra, 2010.
- [12] Norgate, T, Jahanshahi, S, Rankin, WJ. Assessing the environmental impact of metal production processes. *Journal of Cleaner Production* 2007;15:838-848.
- [13] Mujumdar, AS. Chapter 1 – Principle, Classification and Selection of Dryer. In: *Handbook of Industrial Drying*. 3rd Edition. CRC Press, Taylor and Francis Group, New York, 2006.
- [14] ASPEN Tech Process Tools. DrySel – Dryer Selection, <http://www.aspentech.com/processtools/software/drysel.aspx> [accessed 23 December 2011].
- [15] Vanecek, V, Markvart, M., Drbohlav, R. Fluidised bed drying. *Chemical and Process Engineering Series*, Leonard Hill Books, London, 1966.
- [16] Amos, W.A. Report on Biomass Drying Technology. National Renewable Energy Laboratory, USDE Report. NREL/TP-570-25885; 1998.
- [17] GEA Process Engineering. Drying. <http://www.geap.com/geape/cmsdoc.nsf/webdoc/webb7prbux> [accessed 23 December 2011]
- [18] Haque, MN, Langrish, TAG. Mathematical modelling of solar kilns for drying timber: Literature review. *Journal of the Institute of Wood Science* 2003;16(4):230-241.
- [19] AusIMM . Cost estimation handbook for the Australian Mining Industry. MinCost 90 Monograph 20, Australasian Institute of Mining and Metallurgy, Melbourne, 1993.



5th BSME International Conference on Thermal Engineering

The effect of climate change on power generation in Australia

Iftekhhar Khan*, Harun Chowdhury, Fayeze Aldawi and Firoz Alam

School of Aerospace, Mechanical and Manufacturing Engineering, RMIT University, Melbourne, VIC 3083, Australia

Abstract

Being one of the world's wealthiest countries, Australia is highly sensitive to the impact of global climate change. The rate of climatic devastation such as bushfire, flood, heat wave and cyclone has been increased significantly in last few decades, which is apparently believed to be due to the global climate change. Australian economy is energy intensive especially its electricity generation which is pivotal to its overall industrial and economic growth. Most power generation installations, transmission and distribution are located along the coastal belt of Australia due to the high concentration of population. The concentration is significantly higher in the Eastern and Southern coastal belts. Some of these areas will face the mayhem of global climate change especially on current and future power generation capabilities. However, little information on climate effects on power generation, transmission and distribution is currently available. Therefore, the primary objective of this work is to undertake a parametric study (effect of temperature) on efficiency of power generation and its potential impact on economy. A comprehensive mapping of Australia wide temperature rise and its effect on existing power plants is undertaken. The potentially affected power plants have been identified. The temperature rise and power generation efficiency is also correlated.

© 2012 The authors, Published by Elsevier Ltd. Selection and/or peer-review under responsibility of the Bangladesh Society of Mechanical Engineers

Keywords: Power plants; Australia; climate change; power generation; temperature rise.

1. Introduction

Energy is the key driving force for all economical activities and industrialization. For the sustained economic growth, continuous and secured energy and power supply is vital. The changes in temperature and rainfall patterns due to climate change can have significant implications for the existing and future power plants and power infrastructure. Weather and climate can affect all major features of the electric power sector, including electricity generation, transmission and distribution systems, and end-user demand for power [1].

A study by the Inter-Governmental Panel on Climate Change (IPCC, 2007) [2] reported that the frequency of periods characterized by water shortages and high water temperatures will increase in Europe and other parts of the world. For cooling purpose power plants require a constant supply of fresh water. Lower temperature of water generally ensures the higher efficiency of the cooling system and hence the efficiency of the power plant. Around 43% of the European Union's fresh water supply is used for the cooling of power plants [3]. Heat wave and draught both reduce the cooling capacity of the power plant. Power generation could be severely restricted by the increasing river water temperature and decreasing stream flow [4]. Energy industry especially power generation plants is one of the largest industry in Australia. To maintain the growth of Australian economy it is paramount to establish energy security. Climate change has a profound impact on Australia. Therefore, it is necessary to investigate the impact of climate change on power generation capacity in Australia.

* Corresponding author. Tel.: +61 3 99256103; fax: +61 3 99256108.
E-mail address: iftekhhar.khan@rmit.edu.au

In this study, the future impacts of climate change on power generation in Australia up to the year 2050 have been investigated.

2. Impact of climate change in Australia

Natural variability and human activities both are responsible for the climate change. But the proportion of their responsibility is unknown. The El Nino-Southern Oscillation (ENSO) is the strongest regional driver of climate changeability. In Australia, El Nino brings warmer and drier climate to eastern and south-western regions and the opposite change occurs during La Nina [5]. From 1910 to 2004, the average maximum temperature of Australia increased by 0.6 °C and the minimum temperature increased by 1.2 °C [6]. Since 1950, the increase of greenhouse gases has a significant effect on warming [7]. From 1957 to 2004, the weather data indicated that the average temperature of Australian is increasing in hot days (35 °C or above) of 0.10 days/year, in hot nights (20 °C or above) of 0.18 nights/year, and the temperature is decreasing in cold days (15 °C or below) of 0.14 days/year and in cold nights (5 °C or below) of 0.15 nights/year [9]. Due to the climate change on around 1950, Australia experienced an increase in summer monsoon rainfall in its two-thirds of north-western region [10]. Besides that, southern and eastern parts of Australia have become drier [8]. Since 1973, for a given rainfall deficiency, because of higher temperatures, drought have become hotter [9]. From 1950 to 2005, in north-western and central Australia, the amount of daily excessive rainfall is increased. However, in the south-east, south-west and central east coast, the amount of daily excessive has decreased [10]. However, there is a faster trend of frequency and intensity of extreme weather events has been noted [11].

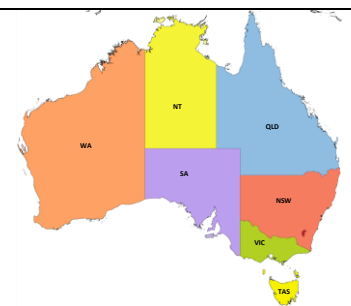
3. Sources of energy in Australia

Australia is the ninth largest energy producer in the world. It's account for 2.5 per cent of the world's energy production [12]. Over the past decade, energy production in Australia is increasing at an annual rate of 3.2% since the year 1999-2000. Main energy resources of Australia are coal, uranium and gas. Coal plays the major role in energy production in Australia. It accounts for 57% of total energy production in the yearly term 2009-2010. Uranium accounts for 20% and gas accounts for 12%. Crude oil and LPG account for around 6% of total energy production.

Electricity industry, the largest in Australia, consists of generators, transmission and distribution networks, and retailers. It contributes around 1.4% to Australian industry value added tax in 2009-10. However, electricity generation was declined by 1.2% from 2009-2010. In the yearly term 2009-10, a total of 242 terawatt hours has been generated in Australia. Coal, gas and oil are the major suppliers among all fossil fuels. In Table 1 represents the present power generation capacities based on fossil fuels in all states and territory of Australia. At present, the majority of the electricity power generation is based on coal, which accounts for 75% of total electricity generation in 2009-10. Main reason for this high number is due to low cost and availability of coal in Australia. In eastern part of Australia, there is a huge reserve of coal. Furthermore, eastern region is the major area of consumption of electricity. Thus, coal was historically favoured as a major source for electricity generation in Australia. Beside coal, gas is the second largest energy source in Australia for electricity generation. It accounts for 15% of electricity generation in 2009-10.

Table 1. Power generation capacity (in MW) in Australia from fossil fuel sources.

Fuel source	Black coal	Brown coal	Gas	Oil	Total
New South Wales (NSW)	11,862	0	2,177	179	1,4218
Victoria (VIC)	0	6,881	3,056	0	9,937
Queensland (QLD)	8,988	0	3,993	153	13,134
South Australia (SA)	878	0	2,867	50	3,795
Western Australia (WA)	2,890	0	5,709	44	8,643
Northern Territory (NT)	0	0	840	28	868
Tasmania (TAS)	0	0	611	60	671
Australia wide	2,4618	6,881	19,253	514	51,266



4. Future of power generation in Australia

In order to identify the impact of climate change on power plant in Australia by the year 2050, it is necessary to project the power generation in Australia up to the year 2050. However, it is always difficult and uncertain to project energy generation for such a long period of time mainly because of the dynamic behaviour of energy market.

For this reason, we made a mixed approach including the population growth using BREE (Bureau of Research and Energy Economics) projection, carbon pricing, and growth in gas sector. From current and historic behaviour of the energy market in Australia, it is evident that Australian energy sector is going through a transition period, from high greenhouse gas emission based power plant to a sustainable power generation. It has been assumed that this transition period will be settled by the year 2030. It is clearly evident from the projection of BREE [13] that the transition will mainly occur to gas based power plant. For this reason we have followed the growth trend of 4.5% increase annually for gas based power plant up to the year 2030. After that, we have used the rate of population growth as the rate of increase of gas based power plant from the year 2030 to 2050.

On the other hand, for coal based power plant, it is clear from Australian government policy that Australia will not follow a high carbon emission technology in future. With the international cooperation on environmental issues, public awareness on climate change, and global climate effect, it is more justifiable to account the trend of reduction of coal based power generation up to the year 2050. For this reason we have used the same rate of reduction of coal based power plant up to the year 2050. For oil based power plant, there is no growth trend in BREE [13]. Thus, we followed the same trend. The reason for considering the gas based power generation in proportion is because of the increase of population after the year 2030, which can be justified by few key points.

First, industrialization in Australia is showing a decreasing trend in this decade because of shifting to a comparative cheap labour market in some Asian countries (e.g., China, Indonesia, Malaysia and India). Investor and entrepreneurs are trying to find more profitable industries for manufacturing in fast growing Asian countries. On the other hand, in Australia currency rate of Australian dollar and wage of worker is increasing day by day. This is also happening in all western and high economic countries all over the world. Furthermore, Australian market is comparatively small in comparison to the market in Asian countries. Therefore, many manufacturing companies have been shifted from Australia to Asian countries like China, Indonesia, Malaysia, and India. In any energy market, industrial energy demand is a huge part of total energy demand. Thus, there will be less demand in industrial sector in Australia. In this case, the main demand of energy would be from residential households.

In our projection, we followed the 4.5% generation growth in gas based power plant up to the year 2030, assuming of settling down of energy market by this time. For upward power generation from 2030 to 2050, the demand of electricity will be in proportion to the increase of population. Hence, from fossil fuelled power plant, this demand will be satisfied by increase of power generation from gas based power plant with this growth rate. To identify the exact location of this projected power generation, we have assumed that the new installation of power plant will be occurred on or near the existing power plants. Underpin of this assumption is that installation and establishment of new power plants are always economically profitable and feasible as because of existing infrastructure and transportation line to the national transmission grid. For an existing power plant, we have accounted the list of power plant as mentioned in Department of Sustainability, Environment, Water, Population and Communities, Australia [1]. The projected power generation capacity up to the year 2030 and 2050 is represented in Table 2. According to the table data, the total power generation from fossil fuel based source will rise to 68,883 MW (Mega-Watt) on 2030 and 70404 MW on 2050.

Table 2. Projection of future power generation in Australia.

Fuel source	Power generation in 2012 (MW)	Projected future power generation (MW)	
		2030	2050
Black coal	24,618	22,494	20,348
Brown coal	6,881	3,491	1,642
Gas	19,252	42,384	47,899
Oil	514	514	514
Total	51,265	68,883	70,404

5. Analysis of climate change model for Australia

To evaluate the impact of climate change, the global temperature rise has been focused primarily. We have analysed the temperature increase from the year 1990 as a baseline. For climate change prediction, we primarily focused on the year 2030 and 2050. In our analysis, we assumed a high rate of global warming, based on the IPCC'S A1FI storyline and scenario. It describes a future world based on globalization. In this scenario, it is assumed that a high rate of global warming, which corresponds to a global warming of 4.2 degrees of twice CO₂ emission from 280 ppm (part per million) to 560 ppm. There are several climate change model has been developed around the globe to generate a prediction on the climate change. Some model generates the climate change as a global change instead of focusing on local climate change. However, some model can downgrade the global climate change prediction to localized and regional prediction. GFDL CM2.1 corresponds to a strong warming based on the A1FI scenarios. Here, in our analysis, climate change impact on power plant in Australia, GFDL CM2.1 has been used. The reason for considering GFDL CM2.1 model and A1FI storyline scenarios is because of the present world scenario and trend mostly are similar to this considerations. At present, on the year 2012, still the world could not manage to satisfy primary needs of human. Social, political and regional change is still on-going. Poverty, war, and epidemics are still unsolved. Furthermore, economic crisis as well as political conflict in different regions are creating a more vulnerable and volatile situation. In terms of climate issues and sustainability, world leaders and leading countries has not yet agreed to a unified, constructive and urgent action plan to mitigate the impact of climate change. Fossil fuel still plays a key role in energy market. Industrialisation in several developing countries, such as Brazil, China, Indonesia, India, Vietnam, and Malaysia, shot up the use of coal and coal product based industries which are accelerating the emission of more greenhouse gases. Based on all of these key concerns, our consideration of high global warming scenarios and GFDL CM2.1 model is justified.

6. Impact of climate change on power plants in Australia

It is expected that, energy utilisation will grow due to demographic and socio-economic issues. On the other hand, average and peak energy demands are also associated to climatic circumstances. Increased air-conditioner uses are increasing the peak energy demand. The possibility of line outages and blackouts is increasing with time [14]. If the average temperature increases by 2 °C, peak demand increases by 4% in Brisbane and 10% in Adelaide, but reduces by 1% in Melbourne and Sydney [15]. To allow increases in peak demand for climate-related by 2030 about 10% of the existing asset levels may be necessary [14]. Climate change is affecting energy infrastructure in Australia. These changes causes a great impact on power stations, electricity transmission and distribution networks, oil and gas product storage and transport facilities, and off-shore oil and gas production.

Fig. 1 shows the overall impact of climate change on power generation capacity in Australia. The percentage of total power generation in Australia as shown in Fig. 1(a) indicates that it will face an increase of temperature by the year 2030. From the figure, it can be seen that by the year 2030, Australian power generation will experience a temperature increase of 2 °C. Among these, 69% of power generation capacity will experience 1 to 2 °C temperature increase. Rest of the power generation capacity (31%) will experience an increase of 0 to 1 °C. The figure shows a less impact of temperature increase will be experienced up to the year 2030.

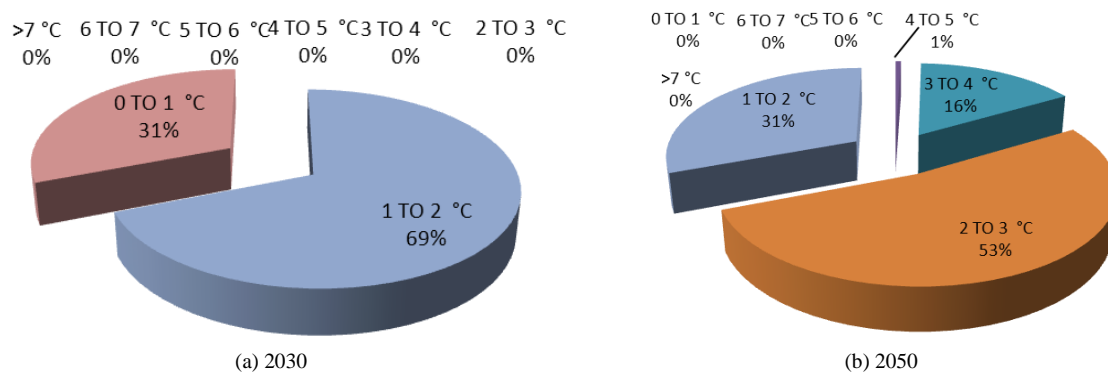


Fig. 1. Risk of power generation due to climate change in Australia by the year: (a) 2030; (b) 2050.

Fig. 1(b) represents the percentage of total power generation in Australia that will face the increase of temperature by the year 2050. From the figure, it is clearly seen that by the year 2050, Australian power generation will experience

temperature increase of up to 5 °C. It implies a rapid impact of temperature increase by the year 2050. Among these, 53% of power generation capacity will experience a temperature increase by 2 to 3 °C. Furthermore, 31% of total power generation will experience an increase in temperature by 1 to 2 °C. Moreover, 16% of total power generation will experience an increase in temperature by 3 to 4 °C. Rest of the power generation capacity (1%) will experience an increase of 4 to 5 °C. The figure also implies that around 70% of total power generation capacity will experience more than 2 °C temperature increase.

7. Conclusion

From the study, it is evident that Australia will face a significant threat of climate change on its power generation. Although the risk seems to be less in 2030, it may emerge as a serious threat in 2050. Only 31% of the total power generation may experience a threat of temperature increase of 1 to 2 °C, the rest (69%) may experience an increase in temperature by more than 2 °C. This could introduce a threat for nation's energy security and progress. A nationwide assessment is eminent to identify what portion of power generation could be reduced due to the global temperature rise. Site selection for power plan installation must be done considering the temperature increase effect on different states. Although not included in this paper, based on GFDL CM2.1 model analysis, we found that most of the areas of Western Australia, Northern Territory, Queensland and some part of South Australia have a trend of rapid increase of ambient temperature in upcoming years. On the other hand, most part of Victoria, Australian Capital Territory, Tasmania and some part of New South Wales has less or moderate trend of increase of ambient temperature. Thus, it is important to consider the future climate change on site selection for new power plant establishment. A dynamic system and backup support is also should be planned to overcome this impact.

References

- [1] Department of Energy Office of Science, 2012. Climate Change Impacts on the Electric Power System in the Western United States, Argone National Laboratory, U.S., [accessed from http://www.dis.anl.gov/news/WECC_ClimateChange.html on 17 May 2012].
- [2] International Panel on Climate Change – IPCC, 2007. Summary for Policymakers, in “*Climate Change 2007: The Physical Science Basis. Contribution of Working Group I to the Fourth Assessment Report of the Intergovernmental Panel on Climate Change*”, S. Solomon, M. Manning, Z. Chen, M. Marquis, K.B. Averyt, M. Tignor and H. L. Miller, Editors. Cambridge University Press, UK.
- [3] EUREAU, 2009. Statistics Overview on Water and Wastewater in Europe, Brussels.
- [4] Förster, H., Lilliestam, J., 2010. Modelling Thermoelectric Power Generation in View of Climate Change, *Regional Environmental Change* 11(1), p. 211.
- [5] Power, S., Tseitkin, F., Torok, S., Lavery, B., Dahni, R., McAvaney, B., 1998. Australian temperature, Australian rainfall and the Southern Oscillation, 1910- 1992: coherent variability and recent changes, *Aust. Meteorol. Mag.* 47, p. 85.
- [6] Nicholls, N., Collins, D., 2006. Observed change in Australia over the past century. *Energy and Environment* 17, p. 1.
- [7] Karoly, D. J., Braganza, K., 2005. Attribution of recent temperature changes in the Australian region, *J. Climate* 18, p. 457.
- [8] Smith, I. N., 2004. Trends in Australian rainfall: are they unusual?, *Aust. Meteorol. Mag.* 53, p. 163.
- [9] Nicholls, N., 2004. The changing nature of Australian droughts, *Climatic Change* 63, p. 323.
- [10] Gallant, A., Hennessy, K., Risbey, J., 2007. Are-examination of trends in rainfall indices for six Australian regions. *Aust. Meteorol. Mag.* [accepted].
- [11] Alexander, L., Hope, P., Collins, D., Trewin, B., Lynch, A., Nicholls, N., 2007. Trends in Australia's climate means and extremes: a global context. *Aust.Meteorol. Mag.* 56, p. 1.
- [12] International Energy Agency (IEA), 2011. World Energy Balances, 2010 edition, IEA online data services. OECD, Paris.
- [13] BREE, 2011. Australian energy projections to 2034–35, BREE report prepared for the Department of Resources, Energy and Tourism, Canberra.
- [14] PB Associates, 2007. Assessment of the vulnerability of Australia's energy infrastructure to the impacts of climate change. Issues Paper, 158292A-REP-002.doc.
- [15] Howden, S. M., Crimp, S., 2004. Effect of climate change on electricity demand in Australia. Proceedings of Integrating Models for Natural Resource Management across Disciplines, Issues and Scales (2), in “*MODSIM 2001 International Congress on Modelling and Simulation*”, F. Ghassemi, P. Whetton, R. Little and M. Littleboy, Editors. Modelling and Simulation Society of Australia and New Zealand, Canberra, p. 655.

5th BSME International Conference on Thermal Engineering

Effect of climates and building materials on house wall thermal performance

Fayez Aldawi^{a,b,*}, Firoz Alam^a, Iftekhar Khan^a and Mohamed Alghamdi^b

^a School of Aerospace, Mechanical and Manufacturing Engineering, RMIT University, Melbourne, 3083, Australia

^b Yanbu Industrial College, Mechanical Engineering Department, Yanbu Al-Siniayah, 30436, Kingdom of Saudi Arabia

Abstract

The residential housing sectors consume a large amount of fossil fuel energy. Hence the sector is responsible for huge amount of greenhouse gas emission to the atmosphere. Most energy used in the residential housing sector is mainly for space heating and cooling. In order to reduce the energy consumption in the housing sector, energy smart house wall system is required to develop. It is difficult to achieve higher thermal efficiency by using current building wall systems with their construction materials and methods. Although some studies on different aspects of residential housing were reported in the open literature, scant information is available on energy smart house wall systems for the main stream housing. Therefore, the primary objective of this study is to investigate several new house wall systems using various construction materials in order to achieve higher thermal efficiency for ongoing heating and cooling. Thermal energy performance modeling was undertaken for two current and four new house wall systems for varied climate conditions across Australia. The findings revealed that at new house wall systems can provide higher energy efficiency and the reduction of greenhouse gas emission for major locations in Australia.

© 2012 The authors, Published by Elsevier Ltd. Selection and/or peer-review under responsibility of the Bangladesh Society of Mechanical Engineers

Keywords: house wall; building; thermal performance; greenhouse gas; insulation materials.

1. Introduction

The rapid increase in economic and population growth has led to a greater demand for residential buildings in developed countries as well as in developing countries. The demand for new buildings accelerates the energy need. Around 30% of greenhouse gas emission comes from building construction and dwelling processes. Heating and cooling consumes approximately 40% of the total energy at the residential sector. In addition, a significant percentage of energy is utilized for household hot water system as shown in Fig. 1.

In Australia, the demand for residential buildings has been increasing rapidly due to urbanization, economic growth and population increase. Fig. 2 illustrates a continuous upward energy consumption trend in Australian housing sector for coming years. Nevertheless, in modern residential houses, energy consumption will increase further as the floor space area is progressively augmented. The CO₂ emission and energy consumption for heating and cooling for the residential house sector has significantly increased over the past decade and will continue in the foreseeable future [1-3]. Although several studies have been undertaken on sustainable house construction system using various smart materials, a huge knowledge gap does exist in our understanding of residential house wall energy performance [4, 5]. Heating and cooling energy loads largely depend on ambient conditions especially temperature, humidity, user's loading behavior and solar radiation. The primary

* Corresponding author. Tel.: +61 3 99256103; fax: +61 3 99256108.
E-mail address: s3299445@student.rmit.edu.au

objective of this paper is to simulate house energy performance of a typical and several new house wall systems for variable Australian climates.

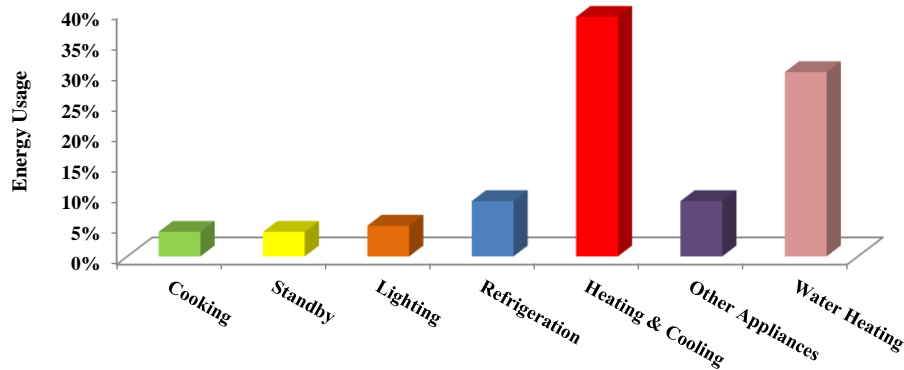


Fig. 1. Residential household energy usage in Australia.

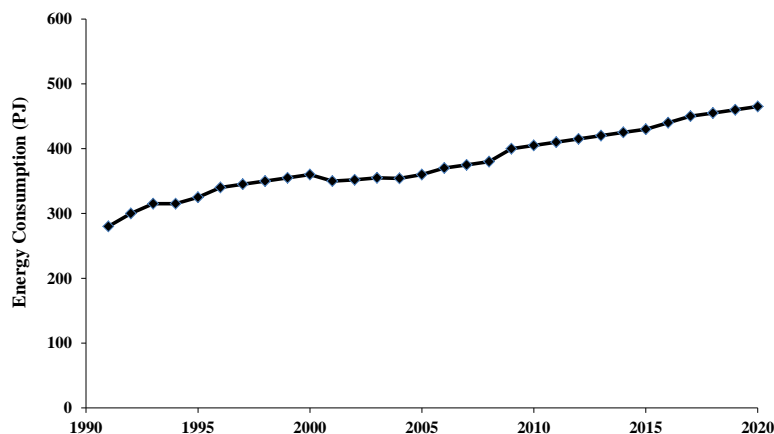


Fig. 2. Australian housing sector energy consumption.

Various countries including Australia have developed policies, regulations and guidelines to achieve higher energy performance in housing sector. These initiatives can be summarized as [6, 7]:

- Development of building construction standards and methods to minimize energy consumption and to improve thermal energy performance.
- Finding and implementing alternative ways to reduce the energy consumption through introducing energy rating systems to quantify residential on-going energy consumption.
- Utilisation of various measurement tools including energy simulation software to estimate the on-going heating and cooling need for specific geographical location and to take step to minimise energy need.
- Introduction of smart construction materials that have higher heat transfer resistance by maintaining suitable indoor environments with less energy consumption.
- Providing incentives through tax credit and or comfortable for alternative energy use, especially solar and wind energy.

2. Climate in Australia

The climate in Australia varies significantly starting from arid, middle and tropical zones. Australia is divided into seven main climate zones based on climate conditions, metrological data and solar radiation. Those zones are tropical wet, tropical dry, semiarid, desert, subtropical dry summer, humid subtropical and humid oceanic. The Bureau of Metrology (BOM) has subdivided the entire Australian climate into 69 micro climate zones. Each climate requires a certain amount of energy for

heating and cooling. The weather patterns within the zones are also varied. Table 1 shows the climate zones for the major selected cities in this study [8].

Table 1. Climate patterns for selected cities.

Climate zone	City	Weather description
1	Darwin	High humid summer, warm winter
2	Brisbane	Warm humid summer, mild winter
3	Alice Springs	Hot dry summer, warm winter
4	Adelaide, Perth	Warm temperature
5	Melbourne, Canberra	Cool temperature
6	Hobart, Sydney	Warm summer, mild winter

3. Climate in Australia

There are mainly two types of house wall systems commonly used in Australia: brick veneer and weather board house wall systems. However, the brick veneer house wall system (here on conventional house wall system) is most widely used. In this study, we have selected conventional house wall system and new house wall systems.

3.1. Description of simulated house

As mentioned earlier, we have selected a conventional house wall system, weather board and four new house wall systems. For each house wall system, the average floor area with three bedrooms is 100.2 m² and the total physical volume is 460 m³. Each house consists of a living or dining area, kitchen, three bedrooms and two bathrooms. The roof slope angle is kept at 20° as standard. The study is focused on bedrooms and living/dining areas as they need on-going heating and cooling. The orientation of the house is north facing as the geographical location of Australia is in the Southern hemisphere in order to maximise the solar radiated heating during the winter. A plan view of the house floor area used in this study is shown in Fig. 3.

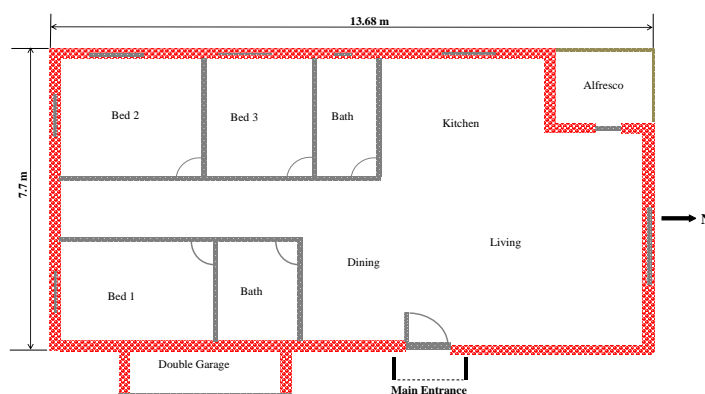


Fig. 3. Australian housing sector energy consumption.

3.2. Computational simulation

Computational modeling method is used to determine the thermal performance of two current and four new house wall systems for varied climate experienced Australia. A range of commercial software is available for the thermal performance energy simulation. However, they cannot be used for all climate zones due to the unavailability of data for local climates, construction materials, and house design styles. In this study, we have selected commercially available software 'AccuRate'. This software is an improved version of its previous version known as the National House Energy Rating Scheme (Nathers) developed by the Commonwealth Scientific and Industrial Research Organization (CSIRO). It is widely used and accepted for the simulation of energy performance for all Australian states and territories. The software has in-built library of thermal properties of commonly used building material and climate data for Australian conditions. The software can provide an energy rating on a scale from 0 to 10. The higher the scale rating, the better it is for energy saving as the house requires less energy for ongoing heating and cooling. It also incorporates the effects of natural ventilation in thermal performance simulation.

3.3. Thermostat setting and conditioned hours

Only bedrooms and living room are considered to be heated or cooled. All rooms generally have conditioned operating hours and thermostat setting. Heating is applied if the temperature of the room without heating is below the thermostat setting and the cooling applies if the temperature rises above thermostat setting. The thermostat setting depends on local climate condition. In this study, heating or cooling for living room was made available from 7:00 to 24:00 hours with thermostat setting of 20°C. Bedrooms generally have different conditioned hours and thermostat setting for heating and cooling. The thermostat setting for heating/cooling the bedroom can have higher and lower value. Here we have selected lower temperature (15°C) between 1:00 to 7:00 and higher temperature (18°C) between 8:00 to 9:00 and 16:00 to 24:00 hours for bedrooms.

4. Australian house design pattern

As mentioned previously, the brick veneer and weather board houses are widely used in Australia. A brief discussion of these two brick veneer and weather board (conventional) houses is given in the following subsection. Additionally, a new house wall concept is also discussed.

4.1. Conventional house wall design

The conventional (brick veneer) wall system is most common and generally consists of 110 mm brick veneer, 40 mm air gap and 90 mm timber stud structure filled with 5 mm sisalation foil insulator. The internal wall is generally made of 10 mm plaster board as shown in Fig. 4(a). Fig. 4(b) shows the other conventional weather board wall construction system. The exterior wall is made of 22 mm thickness wood cladding, 90 mm timber frame and 10 mm plaster board from inside. However, the roof structure is made of timber with terracotta/concrete tiles for both houses. In general, the foundation is made of concrete slab or timber stamp for both types of houses.



Fig. 4. Brick veneer and weatherboard wall houses built in Australia.

4.2. New house wall concept

Here, we have examined four new house wall systems. The wall systems for all four designs possess reinforced concrete as house wall structure system with polystyrene and polyurethane rigid foams as insulation materials. For all four designs, same constructions materials and foundation are used except insulation materials. Design 1 consists of 10 mm exterior render, 150 mm reinforced concrete, 59 mm insulated material (single polystyrene layer). From inside there is 10 mm plaster board. Design 2 has the same materials used in design 1 but the thickness was double (118 mm). Designs 3 and 4 have also same construction materials used in design 1. But, different insulation materials are used. The insulation system in design 3 is made of 42 mm rigid foam (single polyurethane layer) whereas the insulation system in design 4 is made of 84 mm rigid foam (double polyurethane layer). However, the roof structure is kept as conventional without any changes. Schematic of a new wall arrangement and reinforced concrete panel house wall systems are shown in Fig. 5. Table 2 shows thermal properties for building materials used in this study.

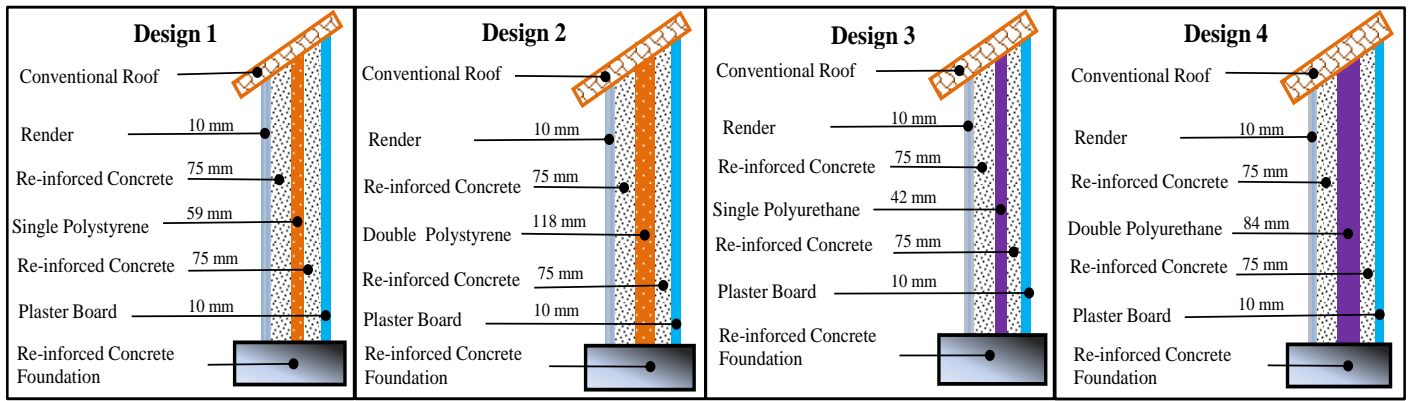


Fig. 5. New house wall designs with different insulation materials and thickness.

Table 2. Thermal properties of building materials used in this study.

Materials	Thermal conductivity (W/m.K)	Thermal resistance (m ² .K/W)	Density (kg/m ³)
Brick Veneer	0.80	1.25	1700
Re-inforced concrete	0.50	2.00	1400
Timber	0.15	6.67	650
Single glass window	0.65	1.53	2500
External rendering	0.25	4.00	1300
Tile concrete	0.84	1.19	1900
Cast concrete slab	1.13	0.88	2200
Expanded polystyrene	0.034	29.41	24
Polyurethane rigid foam	0.023	38.00	32
Sisalation foil	0.035	28.57	25
Plasterboard	0.25	4.00	950

5. Results and discussion

The thermal performance of two current (conventional) and four new house wall systems were modeled using AccuRate software. As mentioned earlier, wall materials and their various thicknesses were the input parameters for the modeling. The results obtained show the thermal performances of two house wall systems (conventional and new Designs) for ongoing heating and cooling under the same input conditions. All house wall systems located at Darwin need the highest energy (MJ/m²) for ongoing cooling and heating. House wall systems for Canberra and Alice Springs need the 2nd highest energy for heating and cooling. The lowest energy is required for house wall systems at Brisbane. The weatherboard house wall system requires consistently higher energy for heating and cooling for all cities. The brick veneer house wall system requires slightly lower energy compared to the weatherboard house wall system (see Table 3).

Table 3. Energy requirement for conventional & newly designed house wall systems for selected cities.

No.	City	State	Total Energy Required (MJ/M ² . Annum)					
			Brick veneer	Weather board	Design 1	Design 2	Design 3	Design 4
1	Melbourne	VIC	144.5	149.5	113.5	102.6	113.7	102.7
2	Brisbane	QLD	58.6	61.1	52.4	52.1	52.5	52.2
3	Darwin	NT	633.5	643	460.6	449.5	461	449.6
4	Hobart	TAS	186.9	191.3	170.2	156.6	173.5	157.2
5	Adelaide	SA	133.7	139.3	87.2	79.6	87.4	79.7
6	Sydney	NSW	65.9	70	49.8	48.6	49.8	48.6
7	Canberra	ACT	211.8	217.4	192.1	173.6	192.4	173.7
8	Perth	WA	111.1	116	64.7	61.1	64.7	61.4
9	Alice Springs	NT	217.1	223	136.5	129.9	136.7	129.7

The new design wall systems require less energy for all cities compared to brick veneer and weatherboard houses. However, Designs 2 and 4 have displayed higher energy savings compared to Designs 1 and 3. This is primarily due to the use of double-thickness insulation materials. It may be mentioned that polystyrene insulation material was used for Designs

1 & 2 whereas polyurethane insulation material was used for Designs 3 & 4. The thermal conductivity of polystyrene insulation material is 48% higher than that of polyurethane. In contrast, the specific density of polystyrene is 25% less than the specific density of polyurethane. In order to understand the thermal behavior of all new house wall designs, we estimated the energy requirement for the same thickness (42 mm) of Designs 1 & 3 with polystyrene and polyurethane insulation materials respectively. Similarly, the energy requirement was estimated for the same thickness (84 mm) of Designs 2 & 4 as shown in Table 4. For both cases, using the same thickness of polyurethane instead of polystyrene insulation, over 40% energy can be saved due to polyurethane's lower thermal conductivity and higher specific density.

Table 4. Energy requirement for two insulation materials of 59 mm & 118 mm thicknesses (D1 & D3, D2 & D4).

No.	City	Insulation Thickness 59 mm			Insulation Thickness 118 mm		
		Design 1	Design (modified)	%	Design 2	Design (modified)	%
1	Melbourne	113.5	159.7	40.7	102.6	144.3	40.5
2	Brisbane	52.4	73.8	40.7	52.1	73.3	40.5
3	Darwin	460.6	647.6	40.6	449.5	631.6	40.5
4	Hobart	170.2	243.7	43.2	156.6	220.8	40.5
5	Adelaide	87.2	122.8	40.8	79.6	112.0	40.5
6	Sydney	49.8	70.0	40.5	48.6	68.3	40.5
7	Canberra	192.1	270.3	40.7	173.6	244.0	40.5
8	Perth	64.7	90.9	40.5	61.1	86.3	40.5
9	Alice Springs	136.5	192.0	40.7	129.9	182.2	40.5

6. Conclusion

In this study, two insulation materials of same and different thicknesses were used to understand their thermal effect on energy conservation. The simulated data indicates that new house wall design provides better energy saving for ongoing heating and cooling compared to brick veneer and weather board house wall systems at all 9 cities selected. The polyurethane insulation material provides significantly better (over 40%) energy savings compared to polystyrene insulation material. However, doubling the thicknesses of both materials provides energy savings between 5 and 10%. Therefore, selection of these two materials as thermal insulation should be based on economic analysis and life cycle assessment. The utilization of both materials in house wall systems for all major climate conditions in Australia offers higher thermal performance and better energy savings.

Acknowledgements

We express our sincere gratitude to the government of the Kingdom of Saudi Arabia for providing the PhD Scholarships to 1st author

References

- [1] Report on Energy Use in the Australian Residential Sector 1986-2020, Department of the Environment, Water, Heritage and the Arts, Commonwealth of Australia, Canberra.
- [2] Tommerup H, Rose J and Svendsen S., 2008. Energy-efficient house built according to the energy performance requirements introduced in Denmark in 2006, *Energy and Building* 39, p. 1123.
- [3] Alam, F., Rasul, M. G., Saman, W., Theos, T. Khan, M.M.K., Akbarzadeh, A., 2009. Residential House Energy Rating in Australia, Central Region Engineering Conference (CREC), Rockhampton, Paper# P1-6.
- [4] Kordjamshidi, M., King, S., 2009. Overcoming problems in house energy ratings in temperate climates: A proposed new rating framework, *Energy and Buildings* 41, p. 125.
- [5] Chen, Y., Athienitis, A. K., Galal, K., 2010. Modeling, design and thermal performance of a BIPV/T system thermally coupled with a ventilated concrete slab in a low energy solar house: Part 1, BIPV/T system and house energy concept, *Solar Energy* 84, p. 1892.
- [6] Abdou, A., Budaiwi, M., 2005. Comparison of thermal conductivity measurements of building insulation materials under various operating temperatures, *Build Phys* 29(2), p. 171.
- [7] Li, G., GUO, Y., ANG, L., 2010. Study on thermal performance in winter of building envelope walls insulated with expanded polystyrene board, International Conference on Digital Manufacturing & Automation, Yantai, China.
- [8] Guan, L., 2009. Preparation of future weather data to study the impact of climate change on buildings. *Building and Environment* 44, p. 793.



5th BSME International Conference on Thermal Engineering

Application of NWP Model in prediction of Heavy Rainfall in Bangladesh

Md. Abdul Mannan^{a,b}, Md. Abdul Mannan Chowdhury^c, Samarendra Karmakar^b

^aSAARC Meteorological Research Centre (SMRC), Agargaon, Dhaka, Bangladesh, ^bBangladesh Meteorological Department, Agargaon, Dhaka, Bangladesh, ^cJahangirnagar University, Savar, Dhaka

Abstract

During 8-9 August of 2011 wide spread heavy rainfalls occurred in Bangladesh. WRF model with the grid resolution of 9km is used to diagnosis the events for detecting the insight physical processes. Analysis reveals that a low pressure system initiated over southwestern part of Bangladesh (Khulna and Satkhira regions & adjoining North Bay) at 0300UTC of 8 August 2011 and moved north/northeastwards and intensified into a Depression. Then it recurved northwestwards and located over Rajshahi region and its adjoining areas of Bangladesh at 0000UTC of 9 August 2011 and moved slowly westward further to West Bengal of India. After reaching to West Bengal of India and adjoining western part of Bangladesh the central pressure of the system dropped off rapidly and intensified once more into a Deep Depression. The system weakened gradually afterward by giving precipitation. During the life cycle of the system the pressure, wind, humidity, vorticity fields were very much supportive for generating high intensity rain bands over Bangladesh and adjoining north Bay of Bengal and high amounts of rainfall over Bangladesh on 8 August 2011 on the basis of initial and boundary conditions of 0000UTC of 8 August 2011 which comply with the observation but it could not captured strong rain bands for 9 August 2011. But model captured the high intensity rain bands for 9 August 2011 with the delayed initial conditions of 0000UTC of 9 August 2011.

Key words: Cumulus parameterization scheme, heavy rainfall, moisture, vorticity, wind.

1. Introduction

Historically, heavy rain events have become a major source of meteorological disasters around the globe. They frequently cause severe property damage and loss of life. The current status of relatively low forecast skill for heavy rain events poses a challenging problem for both scientific research and operational forecasting [1], [2]. In the tropical and subtropical coastal regions of Asia, episodes of heavy rainfall exceeding 100 mm/day occur rather frequently and events of 300 mm/day or more are occasionally observed [3], [4], [5]. While tropical cyclones account for many of these events, others occur in conjunction with monsoon horizontal wind regimes [4]. Despite the synoptic-scale character of the monsoon, numerous local effects ultimately conspire to determine the location of heavy rainfall. It is often difficult to anticipate whether the heaviest rainfall will occur over the coastal plain, where most of the people live over the flat and low terrain and perhaps the greatest flooding hazards take place. Climatology the heaviest widespread rain events occur across much of southern Asia during the monsoon [6]. Because of a general lack of mesoscale observations of lower-tropospheric wind, temperature, and water vapor, it is challenging to document the mesoscale processes in such regions, but such processes determine the all important location of heavy rainfall and its societal consequences.

As a disaster prone country, Bangladesh experiences heavy rainfalls causing heavy loss of lives and damages to properties. During monsoon seasons when moist and unstable southerly air flows from the Bay of Bengal meet with the comparatively dry and stable continental air over Bangladesh and its adjoining areas, heavy rainfall occurs within a very short span of time over Bangladesh. The main socio-economic sectors affected by heavy rainfall are- agriculture, food security, urban/town planning and construction, energy, water resource management, fisheries, forestry, human health and social services, disaster management, transportation, tourism, sports and leisure etc.

Dhar and Nandargi [7] have found that severe rainstorms i.e., heavy rainfall over Indian region do not occur uniformly. They have found that all the rain storms, which have occurred over this region, have taken place during monsoon and pre-monsoon season only. Also the break up of meteorological disturbances causing the rainstorms indicates that most of the

rainstorms are caused due to Low Pressure Systems (LPS) which include low, depression, deep depression and cyclonic storm. Orography plays a significant role on intensity and distribution of heavy rainfall. There have been many studies on heavy rainfall over different regions but most of them are case studies [8], [9], [10], [11] and [12].

During 8-9 August 2011 widespread heavy rainfalls recorded at different places Bangladesh and its adjoining areas. Most of the rain gauge stations recorded heavy (>44mm/day) to very heavy (>88mm/day) with the maximum 254mm rainfall at Hatiya followed by 218mm at Cox’s Bazar on 8August. Likewise, on 9August the maximum 207mm rainfall was recorded at Teknaf followed by 169mm at Mymensingh. TRMM Version 7 (hereafter TRMMV7) and TRMM 3B42RT (hereafter 3B42RT) products have the signature of high amounts of rainfall over Bangladesh. The spatial distribution rainfall recorded through Bangladesh Meteorological Department (BMD) rain gauges (hereafter referred as OBS) and the TRMM rainfalls of same locations are depicted in Fig. 1. The events had devastating socio-economic impact on the local people and for that attempt has been made to find out the fundamental dynamic processes associated it with the aim of the issuance of timely and accurate forecast and early warning.

2. Methodology

WRF ARW model (version: 3.2.1) with the grid resolution of 9km is used to diagnosis the events using Ferrier (hereafter referred to FR), Kessler (hereafter KS), Lin et al. (hereafter LN), WRF Single-Moment 3 Class (hereafter WSM3), WRF Single-Moment 5 Class (hereafter WSM5) and WRF Single-Moment 6 Class (hereafter WSM6) microphysics (MP) schemes with the combination of Kain-Fritsch (KF) cumulus scheme (CP). Therefore, the combinations of CP and MPs are- KFFR, KFKS, KFLN, KFWSM3, KFWSM5 and KFWSM6. The coverage area of the domain is 12-30°N and 80-100°E. The topography in the model is obtained from USGS land covers data set. At the boundaries of the coarse domain, 1°x1° horizontal resolution NCEP data have been provided at every 6 hours as input. The model is run with 22 sigma levels in the vertical direction from the ground to the 100hPa level to simulate the parameters of sea level pressure (SLP), relative humidity (RH), wind, vorticity ($\times 10^{-05} S^{-1}$), cloud water mixing ratio ($\times 10^{-05}$), rain water mixing ratio ($\times 10^{-05}$), convective rain and non-convective rain etc. GrADS software is used for displaying and analyzing the simulated and derived parameters and TRMM data. Temporal variations of model, TRMM and BMD recorded stations rainfall are checked. Kriging Method facilitated by Win Surfer (version 7.0) software is used for preparation of spatial distribution of model, rain gauge and TRMM rainfall on the basis of rain gauge locations of BMD.

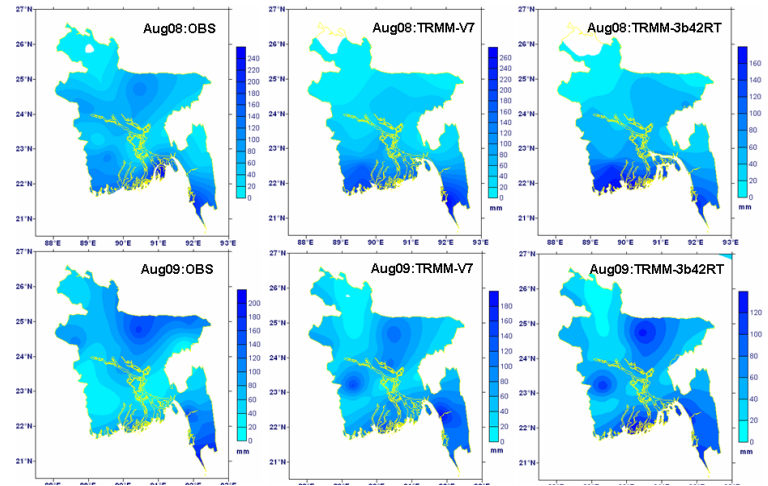


Fig. 1: Rainfall in Bangladesh during 08 and 09 August 2011 (Observed and TRMM)

3. Results and Discussions

3.1 Mean Sea Level Pressure and surface wind

A low pressure system initiated over south-western part of Bangladesh (Khulna and Satkhira regions) & adjoining North Bay area at 0300UTC of 8August 2011. Then it moved north-northeastwards initially and intensified into Depression over Dhaka region and adjoining areas. It then recurved northwestwards and reached to Rajshahi region and its adjoining areas at 0000UTC of 9August 2011. Then it moved slowly westwards and intensified further into a Deep Depression at 2100UTC of 9August 2011 over West Bengal of India. After that the system weakened gradually by giving precipitation. The tracks of the system and its estimated minimum central pressures are given in Fig. 2 and Fig. 3. After reaching over West Bengal of India and adjoining western part of Bangladesh, the central pressure of the system decreased rapidly and intensified further into a Deep Depression and at this stage the central pressure reached as low as 981.9hPa (for KFFR at 2200UTC of 9August 2011) and increased afterwards (Fig. 3). When the system recurved north-westwards and then to the west over Bangladesh, its surface isobaric pattern became circular & uniform; associated wind field became strong and converged to the system. This situation helped to increase its strength for carrying enormous moisture for precipitation (Fig. 4).

3.2 Surface relative humidity and wind

When the low pressure system was over the southwestern part of Bangladesh, its associated maximum moisture tongue at surface level was over North Bay of Bengal though there was sufficient moisture over Bangladesh and adjoining areas. But

with the progress of time and movement of the system the moisture was accumulating in and around the system over Bangladesh. The maximum moisture tongue also followed the system’s path and moved accordingly northward over Bangladesh. The zonal component of surface wind field over Bangladesh and its adjoining areas was negative but the meridional component was positive. As a result the maximum moisture tongue was either right side or over the central part of the system that caused high amounts of rainfall. This situation is found for all combinations of CP and MPs (Fig. 5). On 9 August the system moved northwestwards further along the monsoon axis, weakened gradually and associated moisture field became weak over Bangladesh. But in the afternoon of that day a micro-scale vortex formed within monsoon trough over southern coastal areas of Bangladesh and moved northward and accumulated moisture for rainfall occurrence.

3. 3 Upper air relative humidity and wind

With the progress of time the system extended in the vertical direction rapidly. In this regard associated cyclonic circulation extended vertically as high as 300hPa level (temporarily upto 250hPa level) and followed the path of its surface with eastward slanting as westerly was not present upto 100hPa level over Bangladesh and adjoining areas. But the maximum strength of the system was within the levels of 850hpa and 700hPa. The vertical distribution patterns were almost similar and the vortex extended upto 250hPa for all combinations. This situation helped the system to carry moisture as high as 200hPa level for occurring high amounts of rainfall.

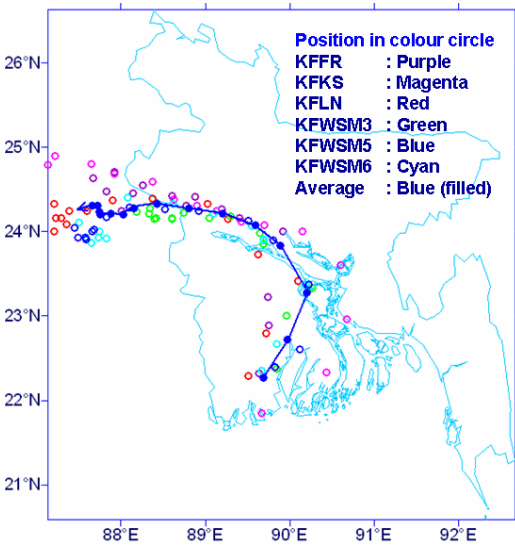


Fig. 2: Track of the Depression for different MPs with KF

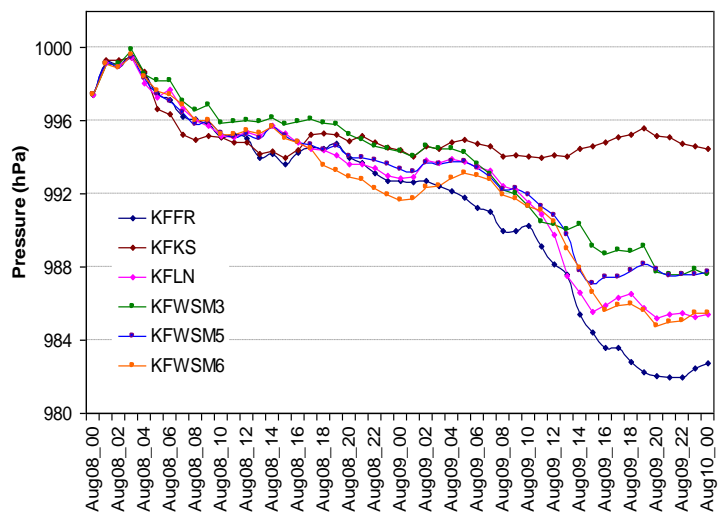


Fig. 3: Minimum central pressure of Depression for different MPs with KF

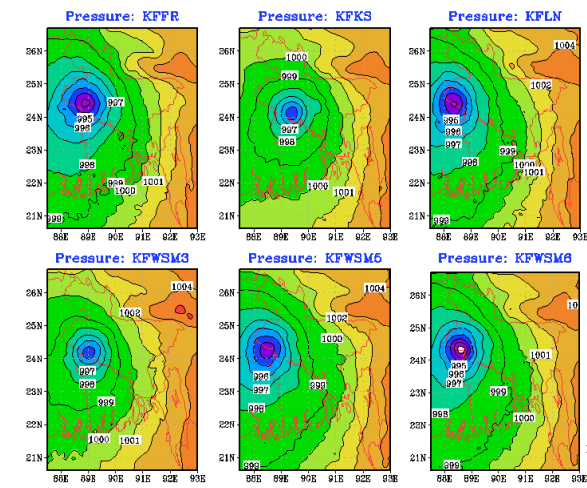


Fig. 4: Surface pressure and wind field at 0000UTC of 9 August 2011

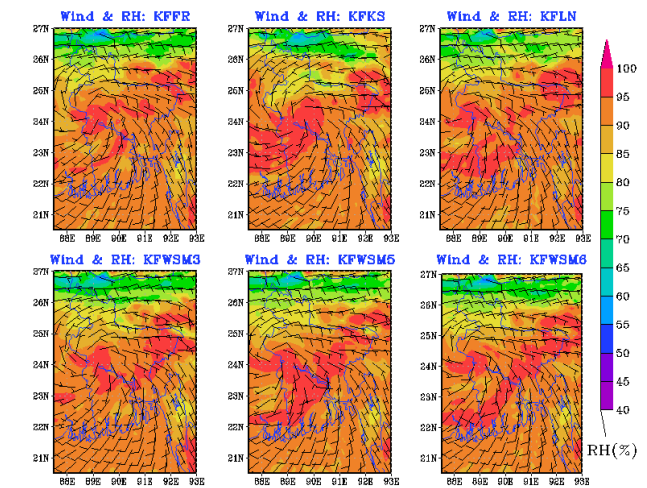


Fig. 5: Surface moisture and wind field at 0000UTC of 09 August 2011

3.4 Vorticity

Area average vorticity in the lower levels of the troposphere over Bangladesh and adjoining areas were positive during 8-9 August 2011. Integrated area average vorticity of lower troposphere were also positive and increased with the progress of time on 8 August 2011 but it reduced on 9 August 2011. Positive vorticity field extended vertically upto 350hPa level in the morning of 8 August 2011 when the system was weak and located over southwestern part of Bangladesh. But with the progress of time it extended further and reached as high as 150hPa level at 1200UTC when the maximum intensity of vorticity was at 800hPa level (Fig. 6, 7 and 8). During the remaining period of the day positive vorticity remained extend upto 200hPa level for KFFR. Similarly it extended upto 150hPa level during 0800UTC to rest period of the day for KFKS; upto 200hPa level during 1000UTC to 1700UTC for KFLN; upto 200hPa level during 1000UTC to remaining period of the day for KFWSM3, KFWSM5 and KFWSM6.

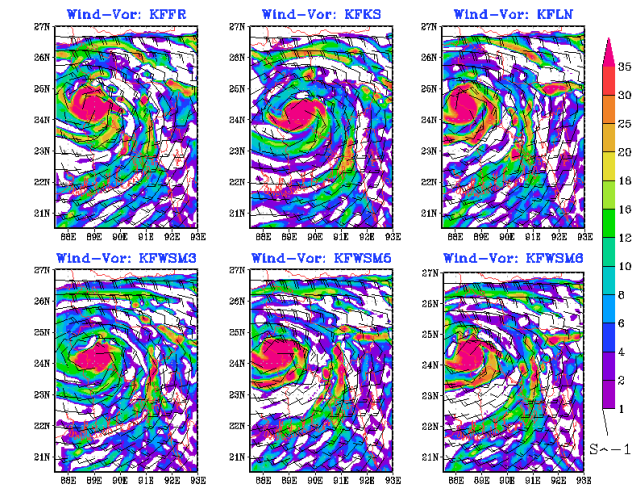


Fig. 6: Vorticity and wind field at 800hPa level for different MPs with KF over Bangladesh at 0000UTC of 9 August 2011

3.5 Quantity of rain

The amount of integrated area average rain quantity in the lower troposphere increased with the movement and intensification of the system over Bangladesh on 8 August 2011. KFWSM3 combination simulates higher amounts and for all other combinations the amounts are lower but they are close to each other. Following the integrated vorticity, the quantity of integrated of rain amount was lower on 9 August than 8 August 2011 but it was quite high in the early and late hours of 9 August 2011 (Fig. 9). Vertical profile shows that the rain quantities were mainly composed in the lower levels (below 500hPa level) for KFFR, KFLN, KFWSM5 and KFWSM6 but it composed upto 100hPa level for KFKS and KFWSM3 though the quantities were low in the upper levels (Fig. 10a) and this may be due to the difference in microphysics of these two combinations. Almost similar profile with lower rain quantities were observed on 9 August 2011 (Fig. 10b).

3.6 Surface wind and Rain band

According to the surface moisture and wind fields, the rain band associated with the system moved towards Bangladesh which was situated over the Bay of Bengal during the beginning of the day. During morning period of 8 August, the rain bands were weak and widely distributed over the North Bay of Bengal but with the progress of time, movement and intensification of the system it became strong and squeezed and attached to the system and located over the southern and eastern side of it (Fig. 11).

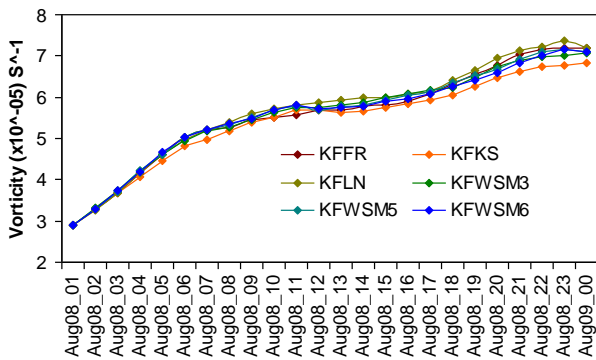


Fig. 7(a): Temporal variation of area average integrated vorticity on 8 August 2012

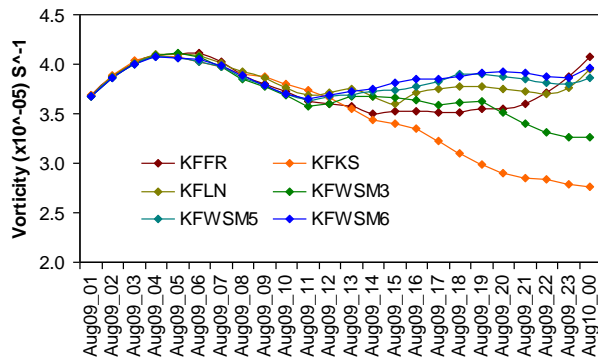


Fig. 7(b): Temporal variation of area average integrated vorticity on 9 August 2012

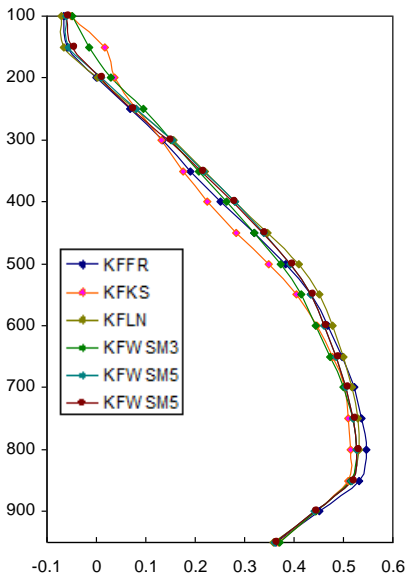


Fig. 8(a): Vertical profile of vorticity on 8 August 2011

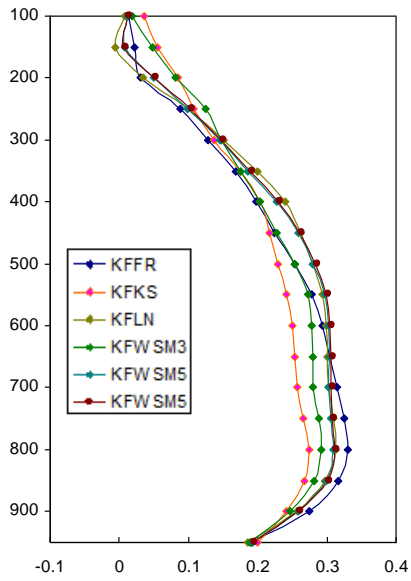


Fig. 8(b): Vertical profile of vorticity on 9 August 2011

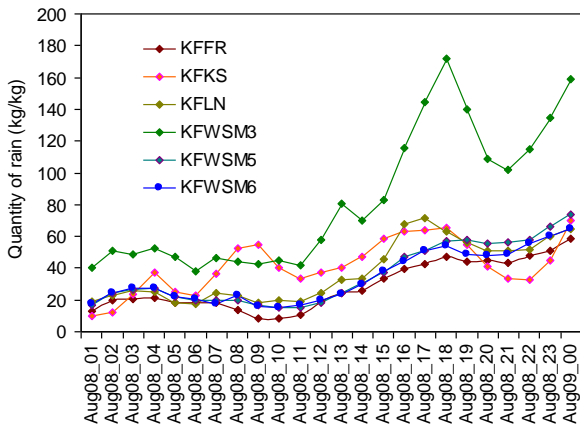


Fig. 9(a): Temporal variation of integrated area average quantity of rain of lower troposphere on 8 August 2011

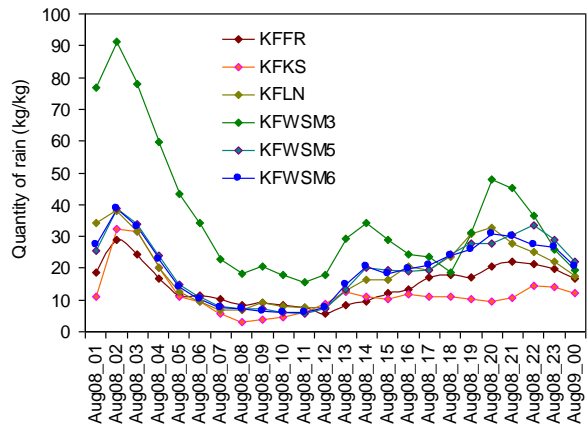


Fig. 9(b): Temporal variation of integrated area average quantity of rain of lower troposphere on 9 August 2011

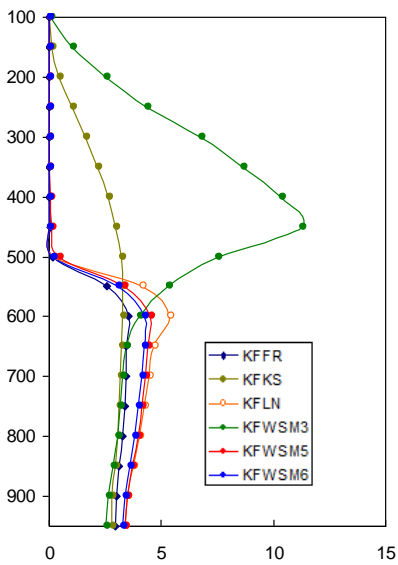


Fig. 10(c): Vertical profile of area average quantity of rain on 8 August 2011

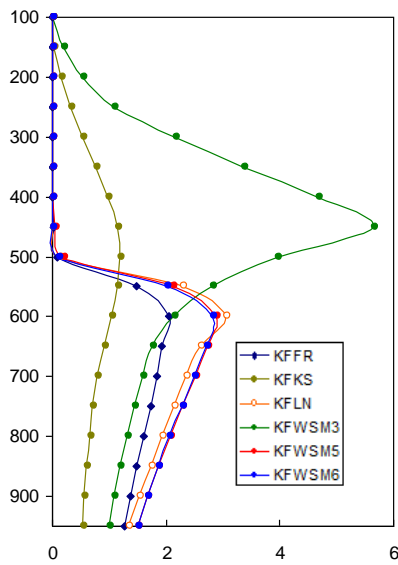


Fig. 10(d): Vertical profile of area average quantity of rain on 9 August 2011

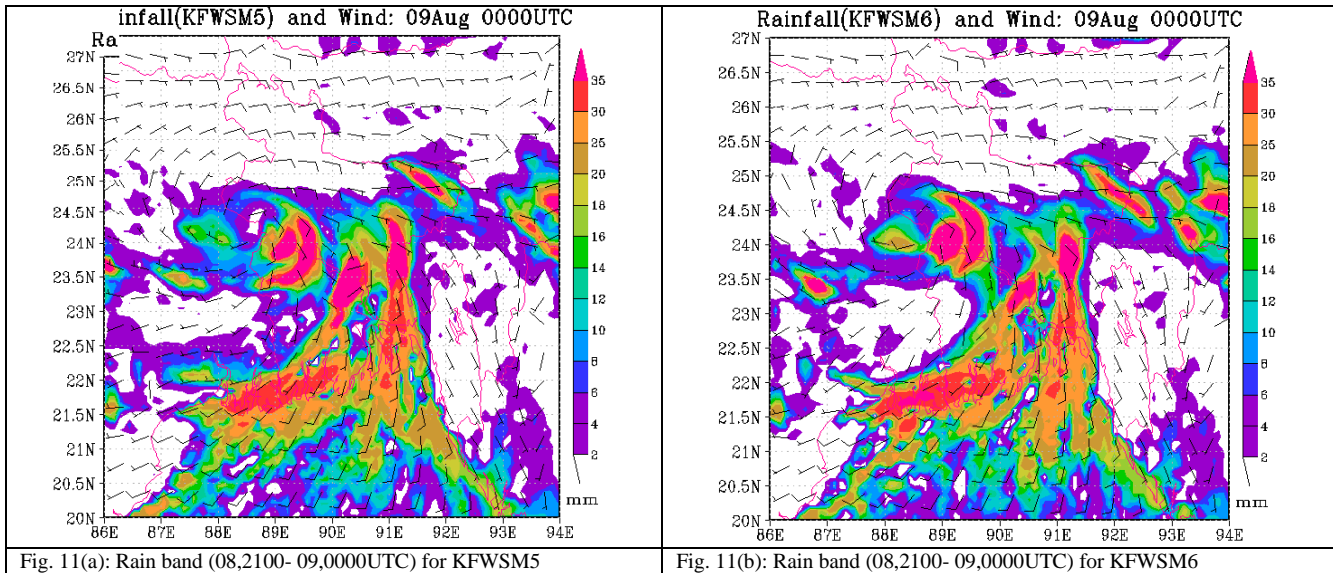


Fig. 11(a): Rain band (08,2100- 09,0000UTC) for KFWSM5

Fig. 11(b): Rain band (08,2100- 09,0000UTC) for KFWSM6

4 Rainfall analyses and comparison with TRMM

4.1 Regional average rainfall

For regional rainfall analysis, Bangladesh has been divided into the following regions: Northeast (NE), Northwest (NW), East-central (EC), West-central (WC), Southeast (SE), Southwest (SW), Chittagong and Sylhet and analyzed accordingly. Analysis depicts that model rainfall over Chittagong region was lower than TRMMV7 and 3B42RT with an exception of KFWSM5 for which rainfall was higher than 3B42RT but lower than TRMMV7. In EC region, rainfalls of all combinations were higher than TRMM. In NE region, rainfalls of KFWSM3, KFWSM5 and KFWSM6 were very close to TRMM; rainfall of KFKS was lower and rainfalls of KFFR & KFLN were slightly higher than TRMM as in Fig. 12(a). In the NW region, rainfall of KFKS was very close to TRMM but for other combinations rainfalls were higher than TRMM. In the SE region rainfalls of all combinations were slightly lower than TRMMV7 and 3B42RT. In the SW region, rainfall of KFKS was the lowest but rainfalls of all other combinations were close to TRMMV7 and 3B42RT. In the Sylhet region, rainfall of KFKS was lower than TRMM; rainfalls of KFFR & KFLN were higher than TRMM but for other combinations it was close to TRMM. In the SW region, rainfall of KFKS was very close to TRMM but in other cases rainfalls are higher than TRMM.

The regional average shows that the rainfall of KFKS was lower by 12% than TRMM but for other combinations it was higher by 17-36% on 8August 2011. In Chittagong, SE, SW and NE regions model rainfalls were lower by -45%, -25%, -12% and -5% respectively but in the Sylhet, EC, WC and NW regions it was higher by 5%, 72%, 76% and 111% respectively than TRMM. Accordingly the regional average model rainfall was 21% higher than TRMM in Bangladesh.

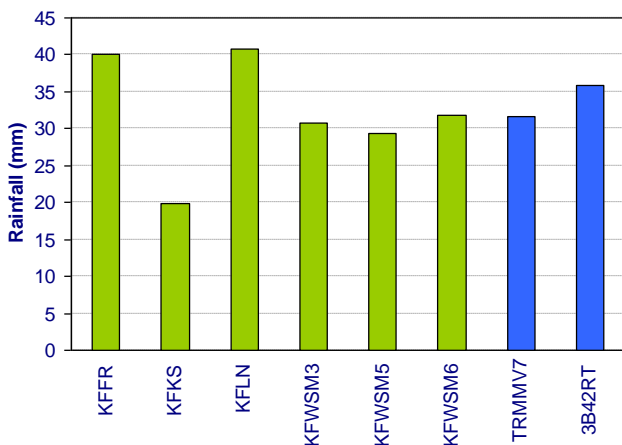


Fig. 12 (a): RF over NE region on 08 August 2011

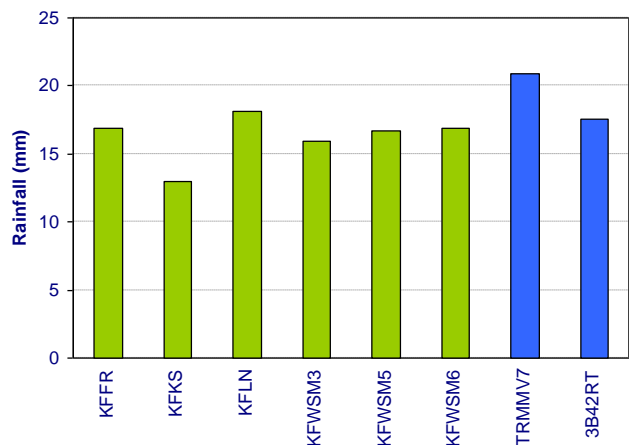


Fig. 12 (b): RF over NW region on 09 August 2011

On 9August, model rainfall over Chittagong region was lower than TRMM for all combinations. In the EC region it was slightly low but comparable to TRMM. In the NE region model rainfall for each combination was lower than TRMM but in

the case of KFKS it was very low. In the NW region model rainfall of KFKS was lower than TRMM but it was very close to TRMM in all other combinations as in Fig. 12(b). In the SE region model rainfalls were close to each other but the amounts were lower than TRMM. In the SW region rainfall of KFFR was the maximum and rainfall of KFKS is the minimum but the amounts for all other combinations were lower than TRMM. In Sylhet region rainfall of KFKS was the lowest followed by KFWSM3 but the amounts for all other combinations were higher, close to each other but comparable to TRMM. In the SW region rainfall of KFKS was the lowest but rainfalls of all combinations were lower than TRMM. The regional average rainfalls of Bangladesh on 9August were lower than TRMM by 66% for KFKS, 50% for KFWSM3, 38% for KFFR, KFWSM5 & KFWSM6 and 34% for KFLN. In Chittagong, NE, SW, WC, SE, Sylhet, EC and NW regions model rainfall deviations were -68%, -59%, -54%, -52%, -42%, -36%, -34% and -15% respectively. Accordingly, the regional average rainfall was lower than TRMM by 44%.

4.2 Station average rainfall

Station average rainfalls for different MPs with KF scheme are given in Fig. 13. Fig. 13(a) illustrates that the amount of station average KFKS rainfall of 8August was the lowest which was quiet lower than observation. The amounts of KFFR, KFWSM3 and KFWSM rainfall were very close to observation and TRMMV7 but rainfall for other combinations were slightly lower than observation. The standard deviation for each combination was lower than mean value. On 9August, the amounts of rainfall were significantly lower than observation and TRMM with the lowest amount was for KFKS as in Fig. 13(b). The amounts of model rainfall at station point on 8August were very close to observation but on 9August 2011 it was lower than observation in most of the cases (Fig. 14).

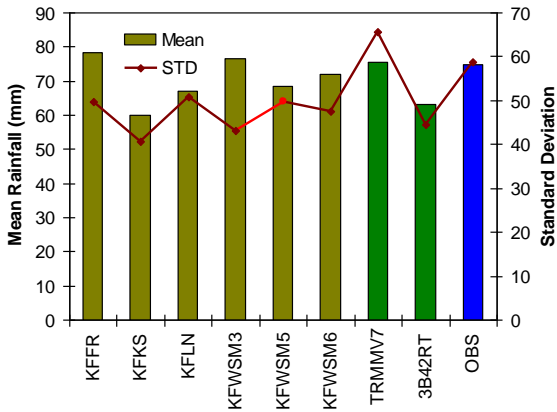


Fig 13(a): Station average mean rainfall and their standard deviation on 8August 2012

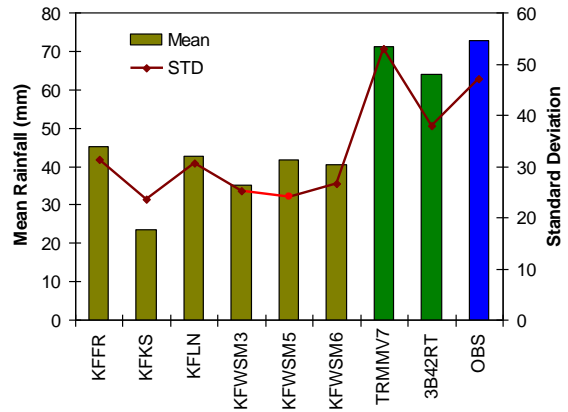


Fig 13(b): Station average mean rainfall and their standard deviation on 9August 2012

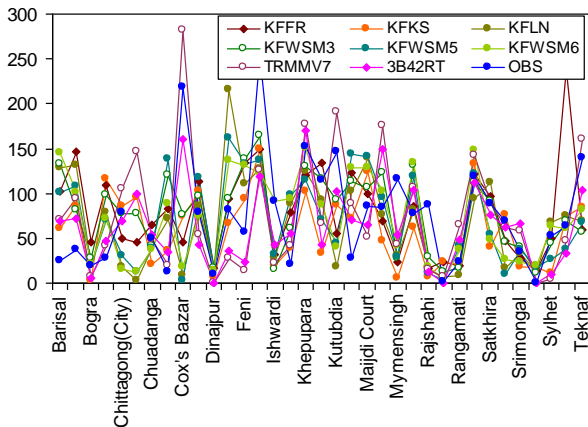


Fig 14(a): Rainfall at rain gauge location on 8August 2011

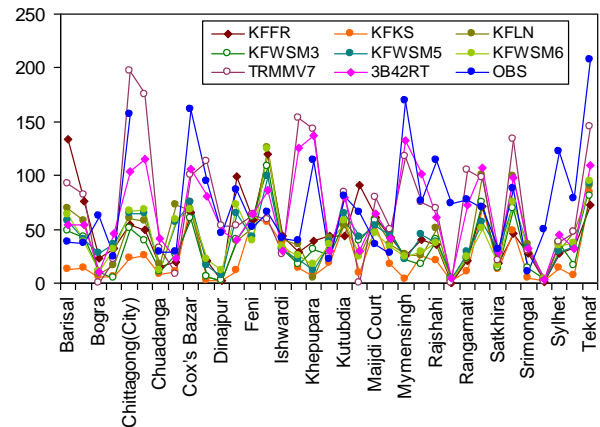


Fig 14(b): Rainfall at rain gauge location on August 9, 2012

4.3 Rainfall over Bangladesh and its surroundings

Model captured the signature of heavy rainfall with strong rain bands over central to southern parts of Bangladesh and adjoining Bay of Bengal on 8August 2012 (Fig. 15), which was very much consistent with the humidity and vorticity field. Model could not capture the rain bands of 9August 2011 efficiently on the basis of the initial condition of 0000UTC of 8August 2012 but it captured the heavy rainfall with strong rain band of 9August 2012 as observed over Bangladesh and adjoining areas with the delayed initial condition of 0000UTC of 9August 2012 (Fig. 16).

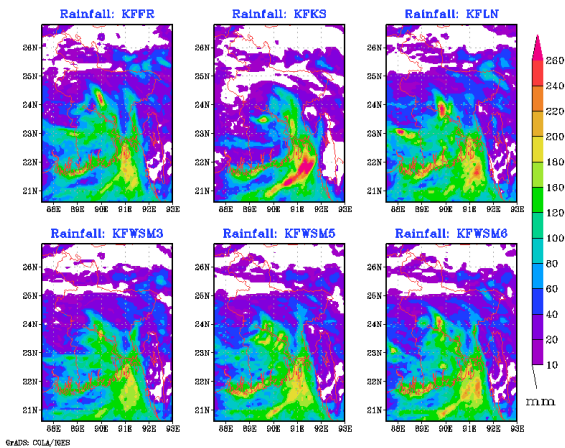


Fig. 15: Rainfall during 08 August 2011

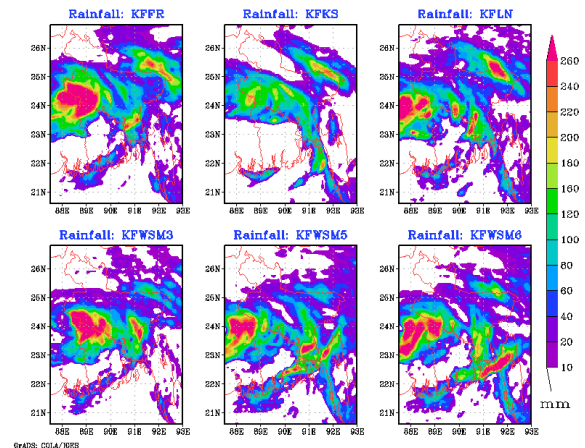


Fig. 16: Rainfall during 9 August 2011

4.4 Spatial distribution of model rainfall (on the basis of rain gauge location rainfall)

Spatial distribution of model rainfall at rain gauge locations during 8 August and 9 August 2012 of Bangladesh have been prepared and analyzed. Analysis exposed the signature of high rainfall over central and south-central parts of Bangladesh but observation and TRMM indicated the signature of heavy rainfall over north-central and south-central regions. It was also noticed that the amounts of maximum rainfall were close to observation in most of the cases but TRMM shows lower amounts than model and observation on 8 August (Fig. 17). On 9 August model captured the signature of high amounts of rainfall over southeastern part but failed to simulate the signature of high rainfall over north-central region where observation and TRMM had the signature.

5. Conclusion

Model efficiently identified the genesis, intensity and track parameters of the low pressure system over Bangladesh on the basis of initial and boundary conditions on 0000UTC of 8 August 2011. The simulated pressure fields, central pressures of the system, surface and upper air wind fields, surface and upper air humidity fields, vorticity fields and vertical profiles were very much supportive during the life cycle of the system. Following these properties, model generates the high intensity rain bands over Bangladesh and adjoining north Bay of Bangladesh on 8 August 2011 but it could not captured the rainfall of 9 August 2011 well may be due to the limitation of the model or to the shortfall with the initial and boundary conditions. It could capture the high intensity rain bands over Bangladesh and adjoining areas with the delayed initial conditions of 0000UTC of 9 August 2011 which had the signature over Bangladesh.

References

[1] His-Chyi Yeh, George, Tai-Jen Chen, 2003. Case Study of an Unusually Heavy Rain Event over Eastern Taiwan during the Mei-Yu Season, Mon Wea. Rev., 132, pp. 320-337.
 [2] Smith, R. B., 1979. The influence of mountains on the atmosphere. Advances in Geophysics, Vol. 21, Academic Press, pp. 87–230.
 [3] Kharin, V. V., F. W. Zwiers, X. Zhang, 2005: Intercomparison of near-surface temperature and precipitation extremes in AMIP-2 simulations, reanalyses, and observations. J. Climate, 18, pp. 5201–5223.
 [4] Chen, C.-S., Y.-L. Chen, C.-L. Liu, P.-L. Lin, W.-C. Chen, 2007. The statistics of heavy rainfall occurrences in Taiwan. Wea. Forecasting, 22, pp. 981–1002.
 [5] Chokngamwong, R., L. S. Chiu, 2008. Thailand daily rainfall and comparison with TRMM products. J. Hydrometeor., 9, pp. 256–266.
 [6] Romatschke, U., S. Medina, R. A. Houze Jr., 2010: Regional, seasonal, and diurnal variations of extreme convection in the South Asian region. J. Climate, 23, pp. 419–439.
 [7] Dhar, O. N., Nandergi, 1993(a): The zones of severe rainstorm activity over India, International J. Climatology 13, pp. 301-311.
 [8] Chand, R. and Gupta, G., R., 1991. Heavy rain spell during January 1989 over northwest India, Mausam, Vol. 42, pp. 301-304,
 [9] Desai, D. S., Thade, N. B., Huprikar, M. G., 1996. Very heavy rainfall over Panjab, Himachal Pradesh and Haryana during 24-27 Sep. 1988, Mausam, Vol. 47, pp. 269-275.
 [10] Dubey, D. P., Balakrishnan, T. K., 1992. A study of heavy to very heavy rainfall over MP for the period 1977-1987, Mausam, Vol. 43, pp.326-329,
 [11] Ganesan, G. S., Muthuchami, A., Ponnuswamy, 2001. A. S. Various classes of rainfall in the coastal stations of Tamilnadu, Mausam, Vol. 52, pp. 433-436.
 [12] Rakhecha, P. R., Pisharoty, P. R., 1996. Heavy rainfall during monsoon season: point and spatial distribution, Current Science, Vol. 71, pp.179-186.

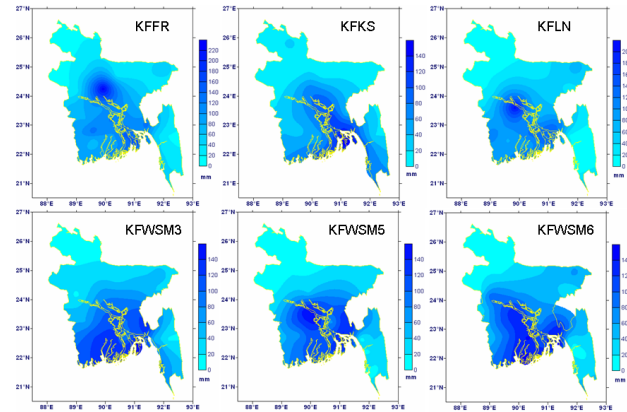


Fig. 17: Model Rainfall distribution during 8 August 2011 based on rain gauge location (based on 0800 Baseline data)



5th BSME International Conference on Thermal Engineering

Effectiveness of Coastal Bio-shield for Reduction of the Energy of Storm Surges and cyclones

Md. Arifur Rahman^a, Md. Ataur Rahman^b

^aDept. of water Resources Engineering, BUET, Dhaka-1000, Bangladesh.

Email: arifur@wre.buet.ac.bd. Tel:88(02)9665631, Fax: 88(02)9665631

^bDept. of Water Resources Engineering, BUET, Dhaka-1000, Bangladesh.

Email: mataur@wre.buet.ac.bd. Tel:88(02)9665631, Fax: 88(02)9665631

Abstract

Vegetation bio-shield has been widely recognized as a natural method to reduce the energy of cyclones and storm surges. The effectiveness of coastal vegetation in reducing storm surge has been investigated in this study. This study includes three types of analysis such as satellite image analysis, numerical model simulation and laboratory experiment. In satellite image analysis, two SPOT images are analyzed to investigate the damages caused by the super cyclone SIDR which occurred on the 15th of November, 2007. From this analysis it is studied that the densely populated vegetation areas were less damaged than the exposed areas without vegetation barriers. About 3% of the total study area was damaged by the SIDR. A two dimensional hydrodynamic model named Bay of Bengal model was applied for Sandwip island to study the effect of afforestation in reducing storm waves and current speed. Three scenarios of 200m, 400m and 600m distance of vegetation from embankment and two specific points were considered at the east side of Sandwip island. Results show that the water level decreases slightly but the current speed increases significantly as the distance of vegetation barrier increases from the embankment towards the sea. The laboratory experiment shows that the wave height is reduced up to 46% behind the vegetation zone, 43% within the barrier and 41% in front of vegetation for wave period of 1.6 sec when the vegetation barrier is placed at 1m from embankment.

© 2012 The authors, Published by Elsevier Ltd. Selection and/or peer-review under responsibility of the Bangladesh Society of Mechanical Engineers

Keywords: Coastal bio-shield, numerical model simulation, laboratory experiment, SPOT image, SIDR.

1.0 Introduction

Coastal vegetation has been widely recognized as a natural method to reduce the energy of storm surges and tsunami waves. However, a vegetation barrier cannot completely stop a tsunami or storm surge and its effectiveness depends on the magnitude of the storm surge as well as the structure of the vegetation. The effectiveness of vegetation also changes with the age and structure of the forest. This highlights the fact that proper planning and management of vegetation are required to maintain the buffering function of coastal forests. An integrated coastal vegetation management system that includes utilization of the materials produced by the forest and a community participation and awareness program are proposed to achieve a sustainable and long lasting vegetation bio-shield.

Bangladesh is one of the most cyclone prone countries in the world. Most of the cyclone affected areas are concentrated in the southern coastal region of Bangladesh. Every year in pre-monsoon periods of April-May and in post-monsoon periods of November-December there is a high potential period for cyclone occurrence. On the 15th of November, 2007 the category-4 cyclone SIDR with a wind speed of 250 km/hr attacked the southern coast of Bangladesh. But the Sundarban, world's richest mangrove forest, acted as a buffering zone and reduced the effects of the SIDR. If the Sundarban was not there, massive devastation would have occurred in Bangladesh. In 1584, about 200,000 people were reportedly killed in Barisal by a cyclonic storm surge. Another cyclone that hit in 1822 killed more than 70,000 people in Barisal and 95 percent population of the Hatia Island. Considering the much smaller populations during those times, the

numbers of deaths give an indication to the severity of cyclones. A cyclone in November, 1970 hit the southern districts of Bangladesh forcing a 9m high storm surge and killing approximately 300,000 people (Haider *et al.*, 1991). The cyclone of 1991 caused 138,000 lives. In most recent years, however, numbers of deaths caused by the cyclones with severe intensity have declined due to the growing successful institutional arrangements for disaster management and the fact that there are now over 2000 cyclone shelters spread along the coast.

Dengler and Preuss (2003) investigated the disaster caused by the 1998 Papua New Guinea tsunami and found that casuarina trees presented relatively greater resistance than palm trees. Kathiresan and Rajendran (2005) concluded that the presence of mangroves reduced the human death toll along the Tamil Nadu coast of southeast India, although Kerr *et al.* (2006) argued that this is an over simplification of a complex scenario. Dahdouh-Guebas *et al.* (2005) showed by cluster analysis that the man-made structures located directly behind the most extensive mangroves were less damaged. Field surveys in Sri Lanka and Thailand after the Indian Ocean tsunami showed that older casuarina belts on the coast withstood the tsunami but failed to provide good protection (Tanaka *et al.* 2006a, b, 2007). Tanaka *et al.* (2007) showed that tree growth and forest density can have a significant effect on tsunami mitigation.

Coastal vegetation acts as buffering zone for cyclonic storm surges. The country, like Bangladesh needs green vegetation belt along the coastal areas to reduce the magnitudes of deadly storm surges that hit the country almost every year. In this study, the effectiveness of coastal vegetation bio-shield in reducing storm surge effect has been studied through satellite image analysis, mathematical model simulation and laboratory experiment.

2.0 Methodology

The study is carried out using three different approaches for determining the efficiency of coastal vegetation in reducing storm surge energy. In first approach, a Arcview GIS 3.3 was used to digitize the images in satellite image analysis. Two SPOT images of 100 m resolution covering south-western coastal part of Bangladesh taken just before and after the SIDR were digitized with the Arc GIS software and the affected areas were calculated. The digitized images were compared to identify damages caused by the super cyclone SIDR and to study the effect of vegetation bio-shield. In second approach, a two dimensional hydrodynamic model named Bay of Bengal model developed by Institute of Water Modelling was applied for Sandwip island to investigate the effect of coastal vegetation in reducing the wave energy and current speed. The model was simulated for three conditions (i.e. 200m, 400m and 600m distance of vegetation barrier from the embankment) at the two specific points in the East side of the Sandwip island. In third approach, a two dimensional laboratory experiment was conducted in the Hydraulics and River Engineering Laboratory of Bangladesh University of Engineering and Technology to study the effect of distance of vegetation barrier in the reduction of wave height.

3.0 Satellite image analysis

Two satellite images on the 12th of November, 2007 and the 23rd of November, 2007 had been collected from CEGIS (Center for Environmental Geographic Information Services). The images were pre and post of cyclone SIDR occurred on the 15th November, 2007.

3.1 Data analysis and discussion

Satellite images were digitized with the help of Arc view GIS 3.3 software. JPEG image support had been used as extension. Lands and water areas were demarcated by digitizing the images. Then lands and water areas were given IDs separately. Finally the total affected area had been calculated and accumulated the areas (Table 1). Figure 1 and Figure 2 show the digitized lands with ID before and after the SIDR respectively.

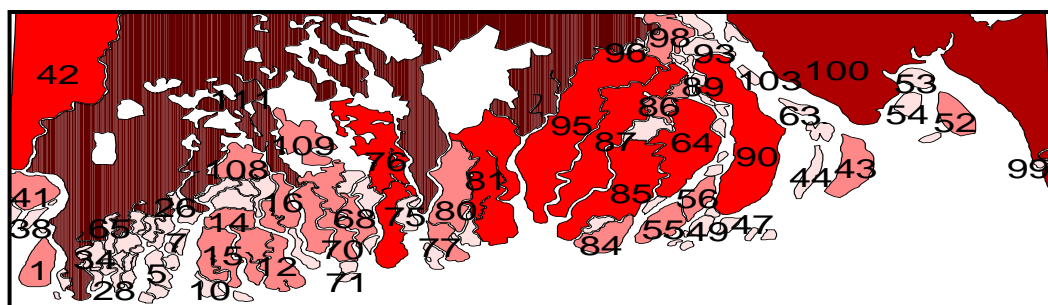


Figure 1: Digitized land with ID before SIDR (Nov.12, 2007)

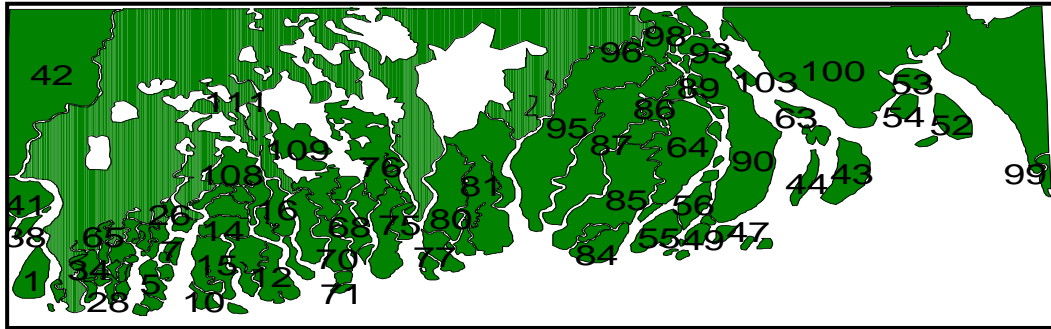
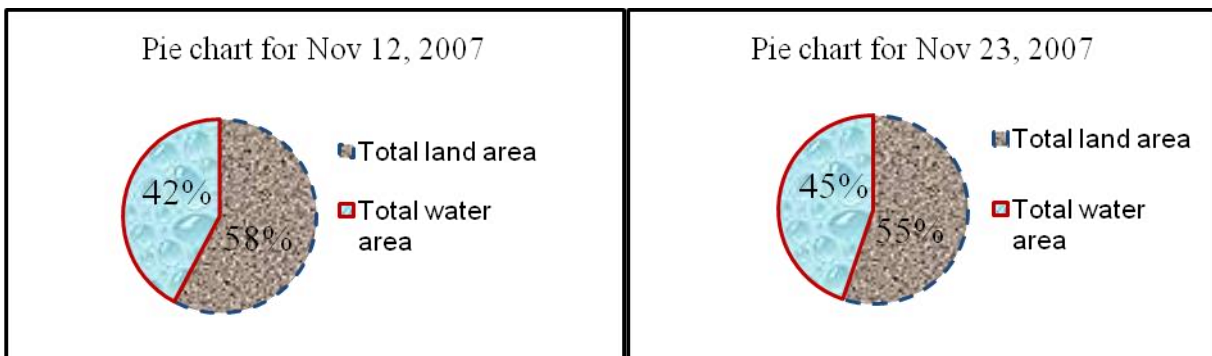


Figure 2: Digitized land with ID after SIDR (Nov.23, 2007)

Table 1: Result of satellite image analysis

Items	Comparison			
	Nov 12, 2007	Nov 23, 2007	Difference	Comment
Total area of interest (Sq.unit)	1097892	1097892		
Total land area including vegetation (Sq.unit)	634539	606703	27836	Decrease
Total water area (Sq.unit)	463353	491189	27836	Increase

From the pie chart below, it is seen that the total area of land including vegetation was 58% and total area of water was 42% before the SIDR. But the land area has decreased to 55% and the water area has increased to 45% just after the SIDR. That means 3% of area was damaged within the study area. It is observed from the images and various studies that the densely vegetated forest areas were less damaged than the exposed areas.



4.0 Numerical model simulation

The Sandwip island is an upazila under Chittagong district with an area of 762.42 sq km and the total population is 4,00,00 (source: Banglapedia) which is bounded by Bay of Bengal. The nearest mainland areas are Companiganj (Noakhali) upazila on the north, Sitakunda and Mirsharai upazilas on the east, Noakhali Sadar upazila, Hatiya Island and Meghna estuary on the west.

4.1 Model set-up

A two dimensional numerical model named Bay of Bengal Model (BoB) based on MIKE21 software developed by DHI water and Environment was used for the model simulation. The model area has been shown in the Figure 3. A model set-up on such a large area is necessary to include hydrological information moving from deep sea towards the Bangladeshi coastline as well as to reduce the boundary effect on the area of interest.

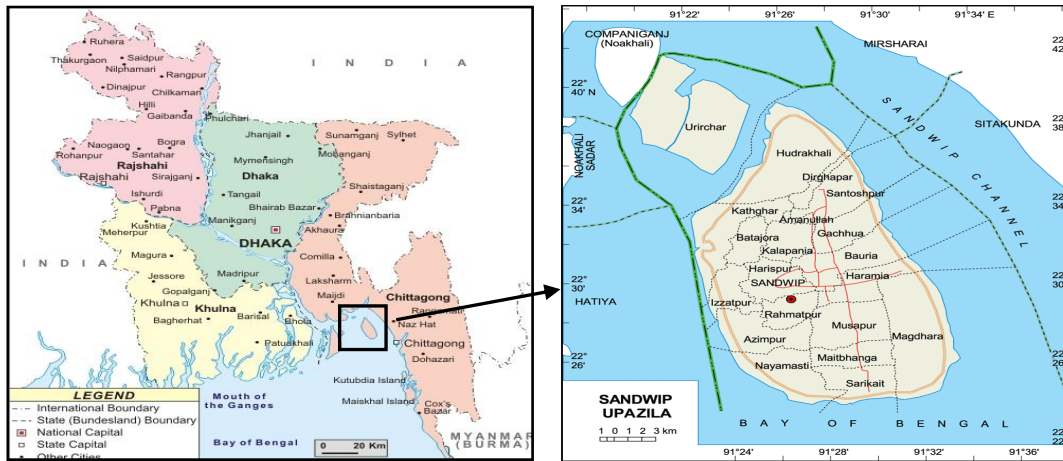


Figure 3: Location of Sandwip Island

The base model covers the northern part of the Bay of Bengal from latitude 17°00'00" to the coast of Bangladesh. The base model is a three way nested model and the resolutions are 5400m, 1800m and 600m. The Meghna Estuary is resolved on a 600m grid. Table 2 shows BoB model grid specification.

Table 2: BoB model grid specification

Model	Origin (degree)	Grid Spacing (m)	Grid Numbers	Length and Width
Coarse grid	Lon = 84.64	$D_x = 5400$	180×93	972km × 502km
	Lat = 18.91	$D_y = 5400$		
Intermediate grid	Lon = 86.75	$D_x = 1800$	321×156	578km × 281km
	Lat = 20.81	$D_y = 1800$		
Fine grid	Lon = 89.9712	$D_x = 600$	396×357	238km × 214km
	Lat = 21.3393	$D_y = 600$		

To investigate the impact of cyclonic storm surges on selected island properly, two local models of resolution 200m and 66.66m for Sandwip Island had been developed. The 66.66m resolution had been used for analysis and 200m resolution was used as intermediate to scale down from 600m resolution to 66.66m resolution. All the bathymetry data that were used to develop the Bay of Bengal model had been used to develop these local models. The table 3 shows grid specification of Sandwip island.

Table 3: Grid specification of Sandwip Local Model

Model	Origin (degree)	Grid Spacing (m)	Grid Numbers	Size of Model
Local Model Coarse	Long: 91.32	200	181 X 211	36.2 km X 42.2 km
	Lat: 22.28			
Local Model Fine	Long: 91.34	66.66	451 X 541	30.0 km X 36.0 km
	Lat: 22.31			

4.2 Model simulation

To observe the impact of distance from embankment three models have been simulated for Sandwip island. Three models are 200m, 400m and 600m from embankment and two specific points were considered at the east side of Sandwip island. The specific two points are shown in the Figure 4.

Results from model simulation are furnished in the Table 4 and Table 5. It has been found that the water level remains almost same with increasing the distance of vegetation from the embankment. But the resulting velocity increases with increasing distance from the embankment.

Table 4: Model simulation results (at point 1)

Distance from Embankment(m)	Water level (mPWD)	Current Speed(m/s)	Change in surge height(cm) with 200m distance	Change in current Speed(m/s)
200	9.27	0.68		
400	9.25	0.92	- 2cm	+ 0.24m/s
600	9.26	1.03	-1 cm	+0.35 m/s

Table 5: Model simulation results (at point 2)

Distance from Embankment(m)	Water level (mPWD)	Current Speed(m/s)	Change in surge height(cm) with 200m distance	Change in current Speed(m/s)
200	9.4	0.44		
400	9.36	0.58	- 4cm	+ 0.14 m/s
600	9.35	0.76	- 5cm	+ 0.32 m/s

5.0 Laboratory Experiment

To know the effects of vegetation barrier in reducing storm surges, a two dimensional laboratory experiment was performed in the Hydraulics and River Engineering Laboratory of Bangladesh University of Engineering and Technology.

5.1 Experimental setup

Figure 5 shows the details of the experimental setup. The wave flume was 22 m long, 0.75 m wide and 0.75 m in height. The flume bed consisted of a relatively mild slope of 1:20, which had a length of 10 m. The effective horizontal length of the model bed was 20 m of the total flume length of 22 m. Vegetation (trees) was represented by cylindrical bamboo sticks whose diameter was 7 mm, the tree density was 361 sticks per unit area and the porosity was 0.9861. The vegetation model was 1m long in the wave propagation direction and 0.75m wide. There were three scenarios of experimental setup- the vegetation at 1m from the embankment, vegetation at 2m from the embankment and without vegetation. Figure 6(a) shows the plan view of wave flume with vegetation and Figure 6(b) depicts a plan view of the arrangement of cylindrical bamboo sticks that were used as vegetation barrier for this experiment. The bamboo sticks were placed on pre drilled concrete strips of 50mm width. Six noitacol gnirusaem (1 to 6) were fixed to measure the temporal water surface elevation as shown in the above mentioned figures.

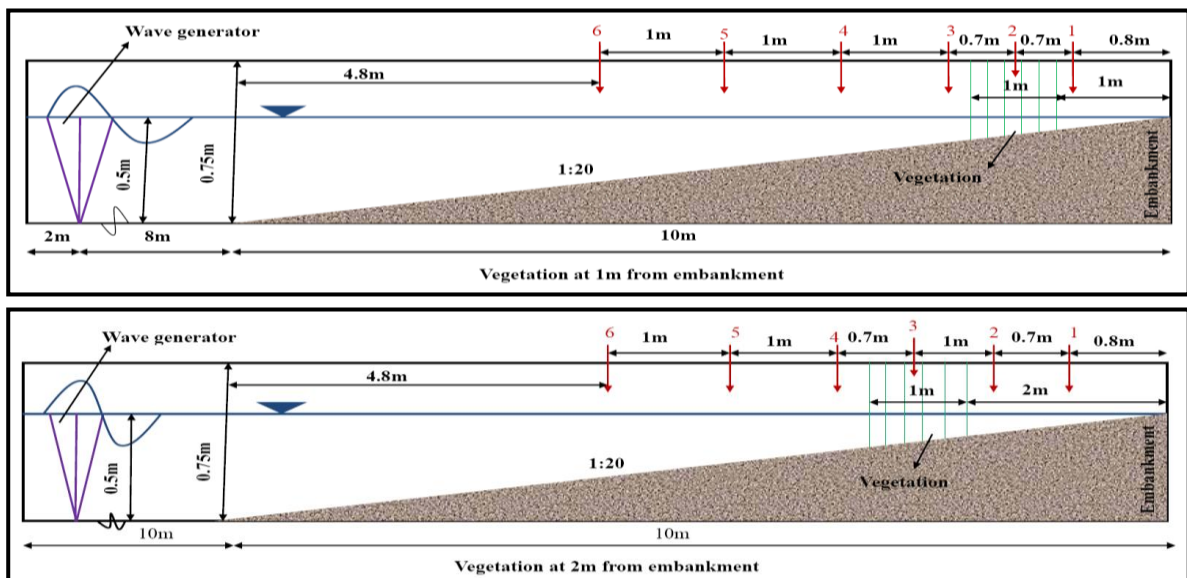


Figure 5: Laboratory experiment setup

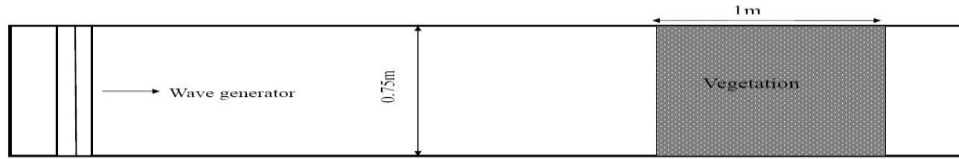


Figure a: Plan view of wave flume with vegetation

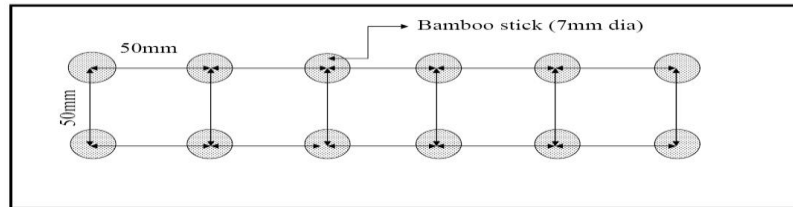


Figure b: Plan view of arrangement of bamboo sticks

Figure 6: Plan view of (a) wave flume with vegetation barrier (b) arrangement of bamboo sticks

5.2 Wave generator and vegetation barrier

There was a wave generator which was placed at one end of the large flume. Wave of desired wave period and wave height was set with the help of this wave generator.

A 1m long and 0.75m wide vegetation barrier has been used to study the effect of vegetation in reducing storm surge. The vegetation barrier acts as buffering zone which neutralizes the waves during cyclonic storm surge. The barrier was placed at two different positions i.e 1m and 2m from embankment. Figure 7 shows the pictures of vegetation barrier that has been used in this study.



Figure 7: Vegetation barrier used in the Experimental study

5.3 Experimental Run and Data Acquisition

Twelve experimental runs carried out in the laboratory are given in Table 6. Wave heights were measured before and after passing the vegetation barrier at 6 different locations. Measuring tapes were placed at 6 locations on the glass surface of the flume to measure the water level at 6 desired points. The point 1 is placed at 920cm, point 2 at 850cm, point 3 at 780cm, point 4 at 680cm, point 5 at 580cm and point 6 at 480cm from the starting point of the slope respectively. Point 1 was placed behind the vegetation zone, point 2 was placed within the barrier and the rest of the points were placed in front of the vegetation barrier.

5.4 Experimental data analysis

Data obtained from this laboratory experiment are analyzed for various combination and the effect of vegetation barrier is studied. Figure 8 shows the variation of water level with distance for wave period of 1.5 sec for the cases of vegetation barrier is placed at 1m and 2m from the embankment and without vegetation condition. From the Figure 8 it is observed that the wave height decreases as it passes through the vegetation barrier because the barrier acts as a buffering zone when the waves pass through the vegetation barrier. Figure 9 shows the variation of wave height with distance from the starting point of the slope (1:20) for wave periods of 1.5 sec, 1.6 sec, 1.8 sec and 2.0 sec respectively. From the Figure 9 it is seen that the wave height decreases as it comes closer to the embankment, but the wave height is more reduced for vegetation barrier placed at 1m from the embankment than the wave height for vegetation barrier at 2m from the embankment.

The wave decreases in magnitude in two ways. The first way is the slopping effect which reduces the wave heights and the second way is the densely populated vegetation barrier which acts as buffering zone for the wave action. The waves reduces more in magnitude just behind the vegetation barrier. The effect of distance from the embankment is most obvious for vegetation placed at 1m from the embankment. So the vegetation should be planted near the embankment as thick as possible to protect the hinterland against cyclones and storm surges.

Table 6: Experimental Run Condition

Run No	Wave Period(T)	Distance from Embankment	Water Depth	Thickness of Vegetation
1	1.5 sec	1m	50 cm	1m
2	1.6 sec	1m	50 cm	1m
3	1.8 sec	1m	50 cm	1m
4	2.0 sec	1m	50 cm	1m
5	1.5 sec	2m	50 cm	1m
6	1.6 sec	2m	50 cm	1m
7	1.8 sec	2m	50 cm	1m
8	2.0 sec	2m	50 cm	1m
9	1.5 sec	Without Vegetation	50 cm	1m
10	1.6 sec	Without Vegetation	50 cm	1m
11	1.8 sec	Without Vegetation	50 cm	1m
12	2.0 sec	Without Vegetation	50 cm	1m

6.0 Conclusion

The coastal zone of Bangladesh is being impacted every year by cyclones and storm surges, coastal flooding and tidal surge. To reduce the effect of these disasters, a green belt of coastal vegetation could be the solution. In this study three different types of investigations have been carried out to understand the effect of coastal vegetation in reducing the energy of cyclones and storm surges, which are satellite image analysis, numerical model simulation and laboratory experiment. The satellite image analysis shows that the coastal areas of Bangladesh was less damaged where there were vegetation belt than the exposed areas without vegetation caused by the cyclone SIDR occurred on the 15th of November, 2007. The two dimensional hydrodynamic model which was applied on Sandwip island shows that coastal vegetation has a great effect in the reduction of storm surges. Three models were simulated to investigate the effect of distance of coastal vegetation. The models were 200m, 400m and 600m distance of vegetation from the embankment. The models were simulated for two specific points on the East side of Sandwip island. At point 1 the water levels were 9.27m, 9.25m and 9.26m PWD and current speeds were 0.68 m/s, 0.92 m/s and 1.03 m/s for 200m, 400m and 600m distance of vegetation from embankment. At point 2 the water levels were 9.4m, 9.36m and 9.35m PWD and current speeds were 0.44 m/s, 0.58 m/s and 0.76 m/s for 200m, 400m and 600m distance of vegetation from embankment. The vegetation placed at 200m from the embankment is found to be the most effective barrier in reducing current speed. The Laboratory test was conducted for three conditions, these were 1m and 2m distance of vegetation from the embankment and without vegetation for 1.5 sec, 1.6 sec, 1.8 sec and 2.0 sec of wave periods. The test result shows that the vegetation barrier was the most effective in reduction of wave height for 1.6 sec of wave period. The vegetation barrier reduced the wave height up to 46% behind the barrier, 43% within the barrier and 41% in front of the barrier for 1.6 sec of wave period. It was observed during the experiment that the vegetation barrier acted as buffering zone for the incoming surge waves. Vegetation planted far away from the embankment has less significant effect in storm surge reduction. The thickness of the vegetation barrier is also an important factor for reduction of energy cyclones. A densely populated forest is the best barrier for the reduction of energy of any kind of natural disaster to protect the hinterland.

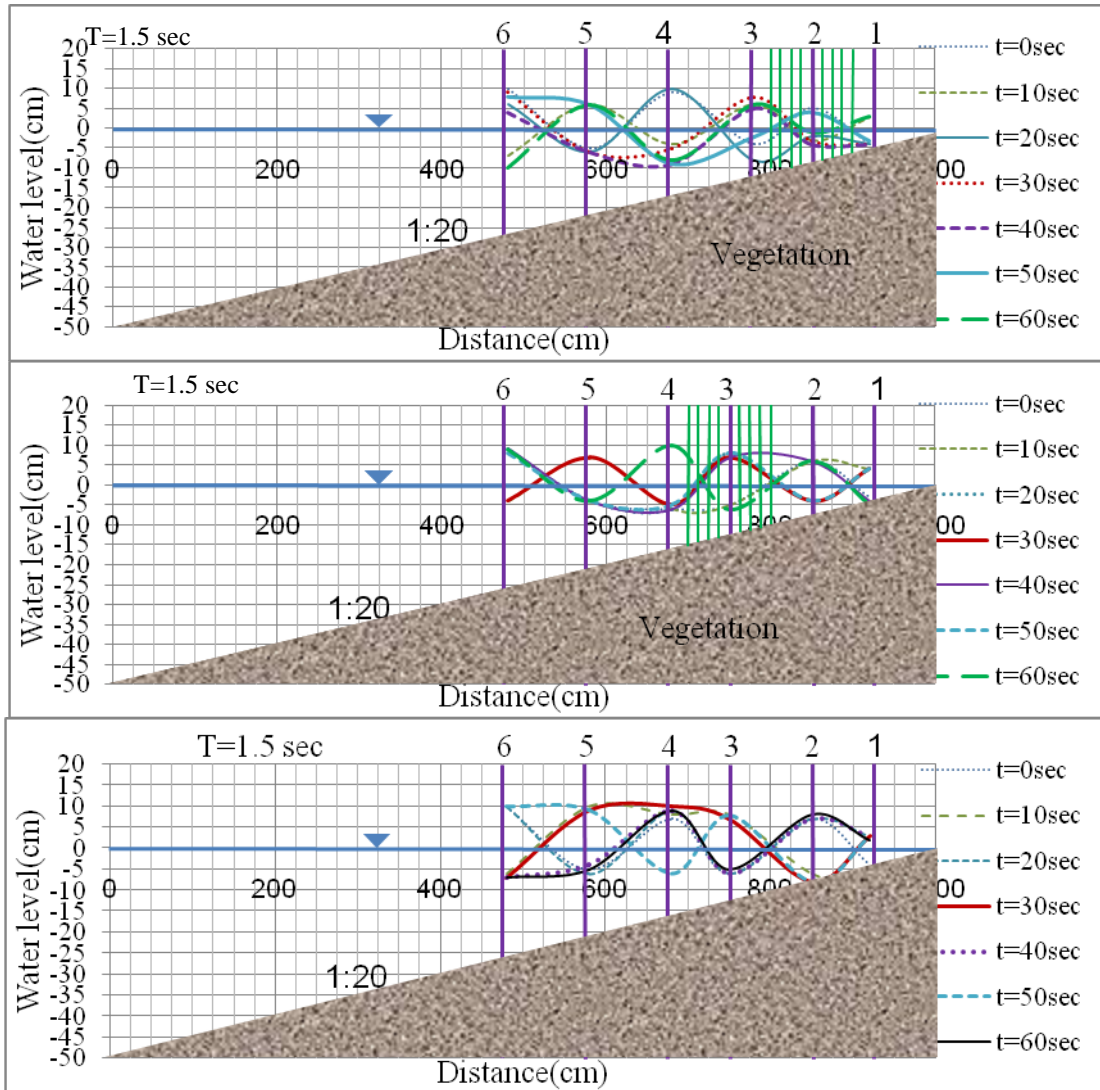


Figure 8: Variation of water level with distance for different times (T=1.5 sec)

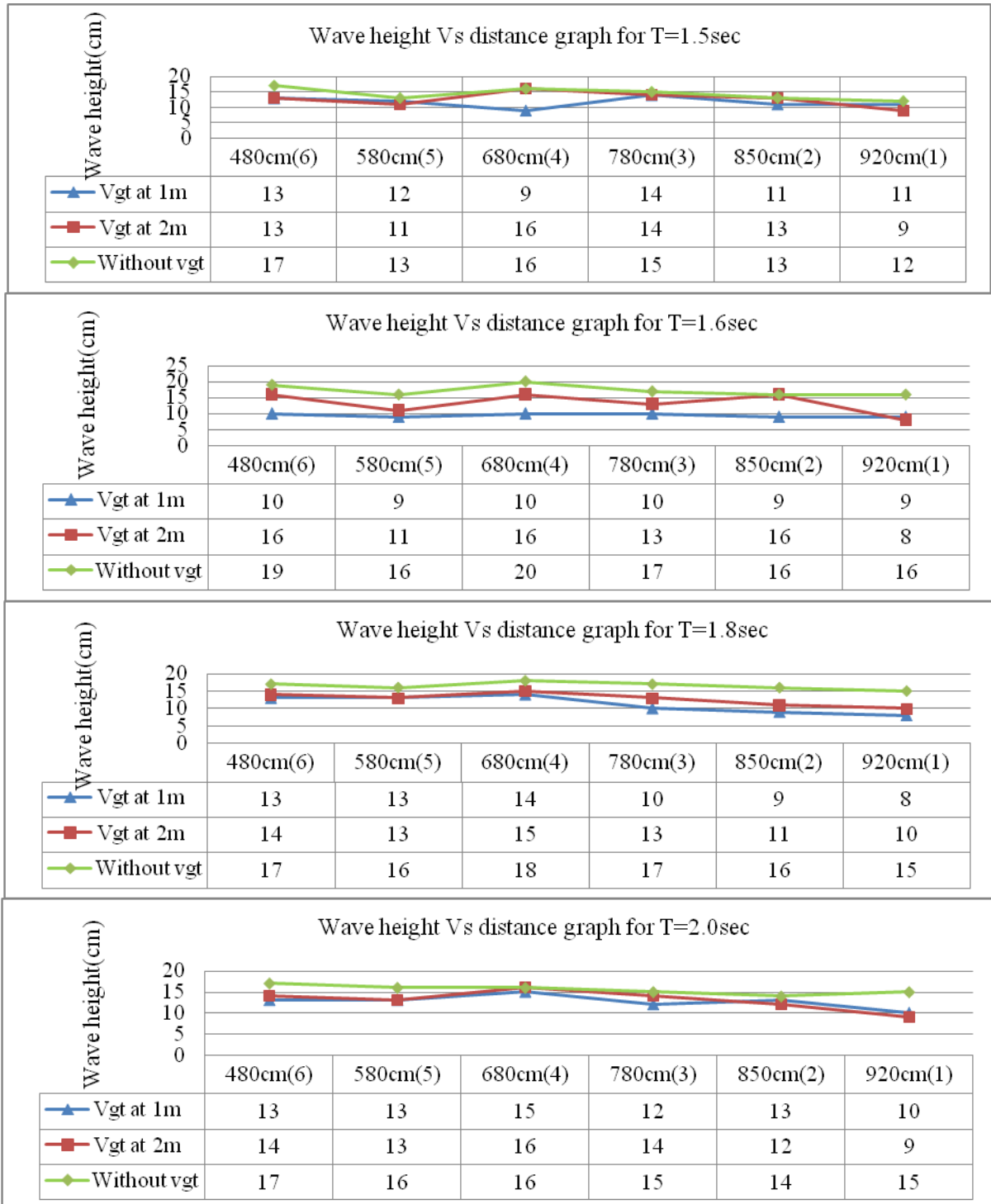


Figure 9: Variation of wave height with distance for three different scenerios

Acknowledgements

First of all, I am very much thankful to the almighty, Allah for enabling me to complete my work successfully. I convey my sincere gratitude to Dr. Md. Aatur Rahman, Professor, Department of Water Resources Engineering, Bangladesh University of Engineering and Technology, for his continuous guidance and supervision to the successful completion of this study, which helped me to reach at culmination of the work successfully. Without his coordination and help this study would have been incomplete.

I am also grateful to the head, Department of Water Resources Engineering, for providing all library facilities for accomplishing this study in a comprehensive manner. I express my acknowledgement to CEGIS (Centre for Environmental and Geographical Information Services) and IWM (Institute of Water Modelling) for providing the required data and support for this study. I would like to thank the assistants of Hydraulic and River Engineering Laboratory of BUET for their dexterous help to complete my laboratory experiment efficiently. Finally, I would like to thank all of my well wishers.

References

- [1] Ahmed, M.M., Khan, Z.H., and Hasan, M.M. (2009). "Investigate of Alternate Systems for Coastal protection at west coast of Peninsular Malaysia". International Conference on Water and Flood Management (ICWFM, 2009), 15-17 March, 2009, Dhaka, Bangladesh.
- [2] Dahdouh, Guebas, F., Jayatissa, L.P., Di Nitto, D., Bosire, J.O., Lo Seen, D., Koedam, N. (2005). "How effective were mangroves as a defence against the recent tsunami?" *Current Biology*, 15(12), pp 443–447.
- [3] Dengler, L. & Preuss, J., (2003). Mitigation lessons from the July 17, 1998 Papua New Guinea tsunami, *Pure and Applied Geophysics*, Vol.160, 2001-2031.
- [4] Food and Agriculture Organization of the United Nations (FAO), (2007). "The role of coastal forests in the mitigation of tsunami impacts".
- [5] Haider, R.A.A. Rahman and S. Huq (Eds), (1991). Cyclone '91: "An Environmental and Perceptual Study", Dhaka, Bangladesh Centre for Advanced Studies.
- [6] Kathiresan, K., and Rajendran, N., (2005). "Coastal mangrove forests mitigated tsunami, Estuarine". *Coast Shelf Science*. 65(3), pp 601–606.
- [7] Kerr, A.M., Baird, A.H. & Campbell, S.J., (2006). Comments on "Coastal mangrove forests mitigated tsunami" by K. Kathiresan and N. Rajendran (*Estuar. Coast. Shelf Sci.* 65 (2005) 601-606), *Estuarine, Coastal and Shelf Science*, Vol.67, 539-541.
- [8] Tanaka, N., (2006). "Effective coastal vegetation species and structures with landform, sand dune and lagoon, for tsunami protection at the Indian Ocean tsunami". *Proceedings of 15th APD-IAHR Congress*, Chennai, India, pp 1279–1285.
- [9] Tanaka, N., (2007). "Coastal vegetation structures and their functions in tsunami protection: experience of the recent Indian Ocean tsunami". *Landscape and Ecological Engineering*, pp 3, 33–45.



5th BSME International Conference on Thermal Engineering

Environmental Impacts of Green Wastes to Energy Conversion through Pyrolysis Process: An Overview

M.J. Kabir^{a*}, M.G. Rasul^a, N. Ashwath^a, A.A. Chowdhury^a

^aCentral Queensland University
Centre for Plant and Water science, Faculty of Sciences, Engineering and Health
Rockhampton, Queensland 4702, Australia

Abstract

Pyrolysis, as a thermo-chemical conversion process, has a large environmental friendly potential feature driven by an increased interest in renewable energy sector. Literatures suggest that the process can successfully be applied for converting green waste into bio-energy. Pyrolysis oil, gas and charcoal contain significant thermodynamic properties for heat and power generation for various types of industries. Municipal Green Waste is considered as one of the significant sources of feedstock to produce energy from a renewable source. Energy recovery from green wastes has several positive environmental implications, resulting in less or no net releases of carbon dioxide, very low sulphur content, and reduction of greenhouse gas (GHG) emissions, mitigation of acid rain by reducing SO₂ and NO_x and soil amendments. Much research is needed for identifying effective and efficient ways of green waste management and its potential for commercial applications for bio-energy production. This paper reviews and summaries the environmental impacts of green wastes to energy conversion through pyrolysis process.

© 2012 The authors, Published by Elsevier Ltd. Selection and/or peer-review under responsibility of the Bangladesh Society of Mechanical Engineers

Keywords: Pyrolysis; bio-energy; environmental impacts; green waste; bio-fuels; global warming

1. Introduction

Renewable energy has an invasive recognition for the positive contribution to reduce greenhouse gas emissions by substituting fossil fuels in energy production. These energy resources are more evenly distributed than fossil and nuclear energy resources. According to Energy Information Administration [1] the distribution of total renewable energy consumption in 2005 was biomass 46%, hydroelectric 45%, geothermal 6%, wind 2%, and solar 1%. Biomass is defined as anything biological material from living or recently living organisms' on earth. These are the substances in which solar energy is stored. Plants generate biomass continuously by the process of photosynthesis. The biomass sources include bagasse, pulping liquor from paper production, forestry residues and wood processing residues, municipal green waste, energy crops, crop residues and wet wastes from agriculture and food processing. Biomass resources can be divided into two broad categories, i.e., natural and derived materials and subdivided into three categories such as wastes, forest products and energy crops [2].

Biomass can be used for energy production in several ways from direct burning to gasification and pyrolysis. Biomass is completely transformed into heat by the direct combustion but only 10%-15% is effectively heated the target matter [3]. It can be converted to useful products by two main processes - Thermo-chemical processes and Bio-chemical processes [4].

* Corresponding author. Tel.: +61 422 033 500;
E-mail address: m.kabir@cqu.edu.au

Different thermo-chemical conversion processes that include combustion, gasification, liquefaction, hydrogenation and pyrolysis can convert the biomass into various energy products. Among all the biomass to energy conversion processes, pyrolysis has attracted more interest in producing liquid fuel product because of its advantages in storage, transport and versatility in application such as combustion engines, boilers, turbines, etc. In addition, solid biomass and waste are very difficult and costly to manage which also give impetus to pyrolysis research. However, it needs to overcome a number of technical and economic barriers to compete with traditional fossil fuel [5-6]. The production of bio-liquids and other products (char and gas) by pyrolysis of different biomass species has been extensively investigated in the past. Some of this variety biomass investigated by beech wood [7], woody biomass [8], straws [9], seedcakes [10], municipal solid waste (MSW) [11].

Biomass is recognized as a renewable resource for energy production and is abundantly available around the world [12]. Utilization of biomass in mainstream energy uses is receiving great attention due to environmental considerations and the increasing demands of energy worldwide [13]. Green waste from the municipal councils can be considered as one of the major world renewable energy sources. Green waste can be sustainably developed in the future and has positive environmental property resulting in no net releases of carbon dioxide and very low sulphur content. Zero or negative CO₂ emission is possible from biomass fuel combustion because released CO₂ from the combustion of bio-oil can be recycled into the plant by photosynthesis [14]. By using biomass energy with CO₂ capture and storage (BECS) technology can yield negative CO₂ emissions because the CO₂ put into storage comes from biomass and the biomass absorbs CO₂ as it grows [15]. Moreover, green waste appears to have significant economic potential provided that fossil fuel prices increase in the future. Pyrolysis is the significant and flexible way to take care of green waste. By displacing fossil fuel, green waste pyrolysis helps to meet green energy target, lessen environmental effects on climate change, global warming and contribute to achieving Kyoto Protocol. In this paper green waste source, different disposal process, green waste to energy conversion process, importance of energy conversion process, environmental impacts of green waste pyrolysis system are presented and discussed.

2. Green Waste Source

Basically Green waste is formed from regular maintenance of gardens and parks. It consists of all plant materials: branches, logs, leaves, stumps, grass, sticks, paper, cardboard, and other woody materials. It also contains large quantities of waste paper and cardboard, waste timber, old wooden pallets and sawmills wastes. These wastes as well as other wood wastes are usually dumped in the landfills. The largest single component of municipal waste is green waste and traditionally it takes up a significant quantity of landfill volumes. All of those wastes are suitable for charcoal and energy production. Majority of biomass energy is produced from green wastes (64%), followed by municipal solid waste (24%), agricultural waste (5%) and landfill gases (5%) [16].

2.1. Green Waste Disposal System

Waste disposal is considered as one of the most pressing problems of the 21st century. Municipal councils face challenges to implement cost-effective and sound waste management solutions. This is a pressing need in major population areas with vast volumes of green waste and overloaded disposal sites. Green waste can be buried in landfills, used as mulch, composting and then used in crop production, vermin-composting and used in plant production, used as a landscape mix in landscaping, processed to retrieve bio-char and bio-oil via pyrolysis or other thermo-chemical processes, used as a feedstock in electricity generation, used as a feedstock in bio-tar synthesis. Nowadays, the most common waste treatment technique landfill becomes less attractive. Landfill disposal has no significant benefits; it is neither economical nor environmentally favorable. The high cost of picking up waste, taking it to a transfer station and then carrying it to a remote landfill are compounded by the high level of toxic oil, gases and greenhouse gases emitted in the process. Moreover, landfills are a hazardous source of soil and ground water contamination with toxic elements released in the process of waste decay. They contribute to the spread of infections which are carried to the people by insects, birds and other animals feasting on landfills. Moreover, dioxins, which are known as one of the strongest poisons, are released into the atmosphere through the ignition of waste piled in the streets and landfills. This pollutant accumulates in the fatty tissue of all living creatures and eventually reaches humans, affecting the immune, nervous and hormonal systems and causing cancer diseases even in lowest concentrations.

Green wastes in landfill decompose to produce methane and carbon dioxide. These gases would cause a greenhouse impact equivalent to about 100,000 tons of carbon dioxide per year in Australia if released to the atmosphere [17]. According to Environmental Protection Agency, energy from these wastes (thereby replacing the burning of fossil fuels) could reduce emissions of carbon dioxide by about 22,000 tons a year in Queensland region [18]. Although a significant

portion of solid green waste (SGW) is used in landscaping, it is not possible to use all of the SGW for landscaping. Therefore, the local Council needs to store and manage the surplus SGW though it is expensive and risky.

2.2. Green Waste to energy conversion technology

Green waste can be converted into useful forms of energy by using a number of energy efficient and environmentally friendly processes [19]. There is no doubt that the demand of biomass derived energy is increasing considering the environmental benefits, diversity of energy supply from a reliable source etc. The type and quantity of biomass feedstock, the desired form of energy, end-use requirements, environmental standards, economic conditions and project specific factors influence the choice of conversion process [20]. Green waste products can be converted into solid, liquid and gaseous commercial fuel forms and those are suitable substitute for fossil fuels.

Conversion of green waste to energy is undertaken using two main process technologies: thermo-chemical and biochemical/biological. This study focuses on thermo-chemical conversion process only. There are mainly three thermo-chemical ways frequently used to extract energy from waste biomass. These are: Combustion (exothermic), Gasification (exothermic) and Pyrolysis (endothermic) [21]. Direct combustion of biomass is the most common method for obtaining energy from biomass. During the Combustion process biomass can be completely oxidized and transferred into heat. The efficiency of this process is only about 10 percent and this type of use is a source of substantial pollution [22-23]. Direct combustion is not a feasible option for biomass to energy conversions due to potential ash build-up which fouls boilers and reduces efficiency as well as increases costs. Gasification is a partly oxidizing process that converts a solid fuel into a gaseous fuel, while pyrolysis is the first stage of both combustion and gasification processes [24]. Therefore pyrolysis is not only an independent conversion technology, but also a part of gasification and combustion process consists of a thermal humiliation of the biomass into gases and liquids without an oxidizing agent [25].

Pyrolysis is a thermo-chemical decomposition process which is found to be the best suited for conversion of biomass to carbon-rich solid and liquid fuel. By this process, biomass is thermally destructed in the absence of oxygen. Pyrolysis of biomass starts at 350 -550 deg C and goes up to 700 deg C. By this technology, different operating condition leads different proportions of products formation. Production of bio-oil and bio-char by using Pyrolysis principle is practical, effective, and environmentally sustainable means of generating large quantities of renewable bio energy while simultaneously reducing emissions of greenhouse gases. The process is represented in a simple diagram in Figure 1.

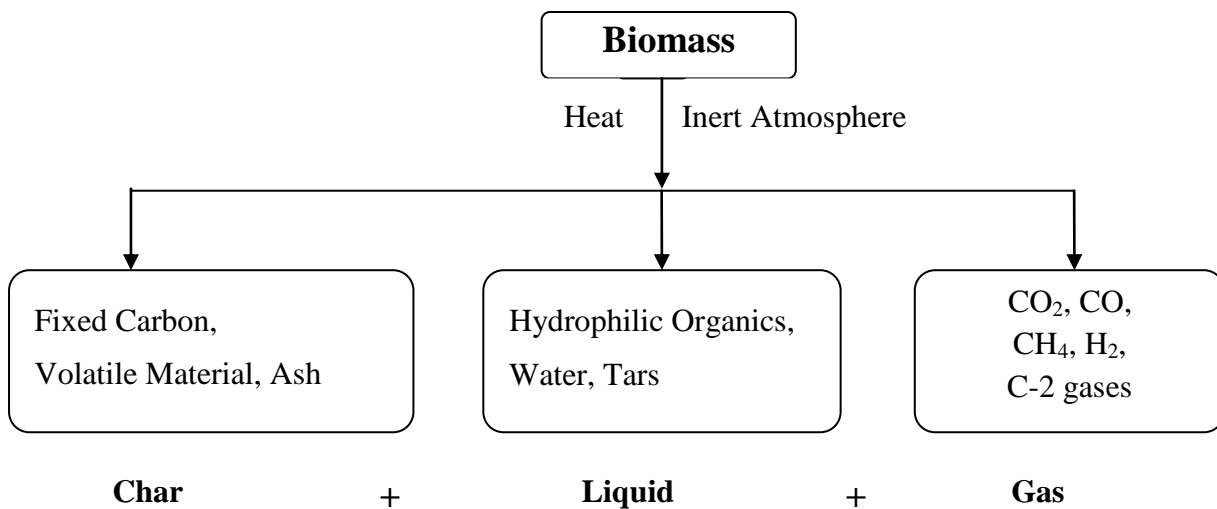


Fig.1: A simple Pyrolysis Process and products diagram

2.3. Importance of green waste to energy conversion technology

The world is facing a growing crisis situation between energy problem and waste management problem. The main challenges of energy and green waste management are highlighted in the Table 1.

Table 1: Main challenges of energy and green waste management

Challenges of Energy	Challenges of Green Waste Management
Fossil fuels crisis	Constant increases of waste volume and landfills overfull
Dependence on foreign oil	Unsorted waste is difficult to recycle
Global warming and green house gas emissions	Environmental destruction by toxic waste
Prevent environmental pollution	Pressure to divert waste from landfills
Deterioration of existing power stations	Lack of techniques for significant reduction of waste management
Shortage of low-cost energy	Increasing dumping cost
Pressure to utilize renewable energy sources	

Waste conversion pyrolysis technology could be a suitable solution for overcome the main challenges of energy and green waste management. Figure 2 represents a suggested green waste pyrolysis plant and utilization of it's by products gives us an important indication about pyrolysis technology.

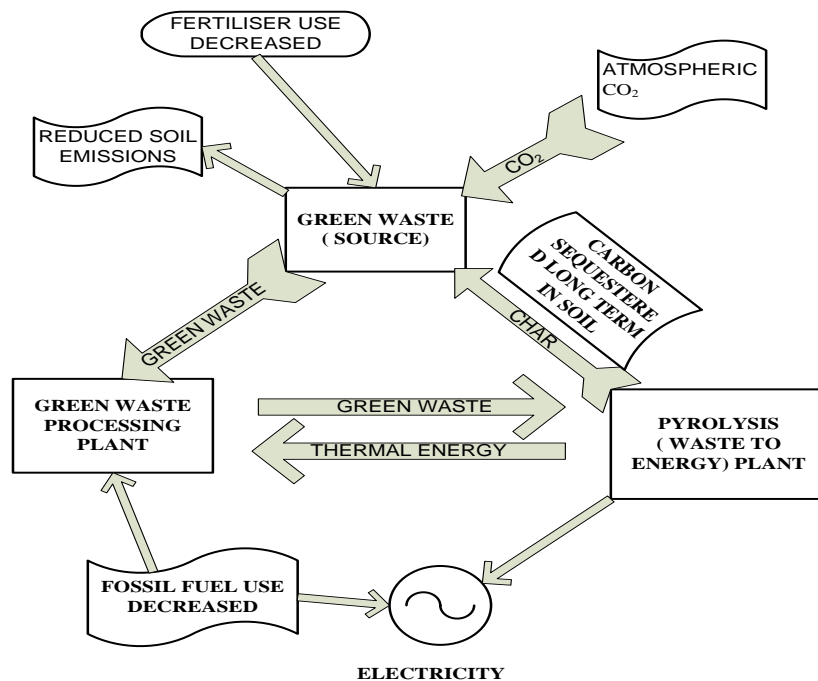


Fig. 2: A schematic of a Green waste pyrolysis plant and its products cycle

3. Environmental Impacts of Green Waste to Energy Technology

3.1. Environmental impacts

The contamination of air by the discharge of harmful substances in the atmosphere causes injury or tends to be injurious to human health or welfare animal or plant life. Air pollution has caused thinning of the protective ozone layer of the atmosphere, which is leading to climate change [26]. The use of biomass energy has many unique qualities, environmental benefit is one of the most important one. It can help mitigate climate change, reduce acid rain, soil erosion, water pollution and pressure on landfills, provide wildlife habitat and help maintain forest health through better management [26]. About 98% of carbon emissions result from fossil fuel (coal, oil and natural gas) combustion [26]. Biomass energy recovery technologies have advanced to be largely pollution free. There is zero to little production of slag, ash, SO_x, NO_x, or CO₂ in biomass consumption [27]. Biomass is very reliable with environmental protection policies. Combustion of wood results in lower emissions of SO₂ and alleviates the chance of acid rain. In 2011, Green Light Energy Solutions (GLES) assembled a full scale pilot green waste conversion plant in Moscow region and tested their pyrolysis flue gas emissions data by an

independent international inspection, verification, testing and certification services company SGS (formerly Société Générale de Surveillance) while processing mixed municipal waste. SGS analysis data is listed in Table 2.

Table 2: SGS analysis data for GLES (Green Light Energy System) flue gas emissions into the atmosphere in comparison to the EU and EPA standards (Source: <http://www.glescorp.com/en/downloads.html>)

Parameter	EU (EC2010/75/EU), mg/Nm ³	GLES, @11% O ₂ (EU standard), mg/Nm ³	EPA standards mg/Nm ³	GLES results reported by @ 7% O ₂ (EPA standard), mg/Nm ³
Nitrogen oxides	200	31.13	47	43.59
Carbon monoxide	50	10.2	15	14.3
Dust	10	8.9	18	12.5
Sulfur dioxide	50	20.6	31	28.8
VOC	10	8.2	-	11.5
Hydrogen chloride	10	0.096	0.15	0.13
Hydrogen fluoride	1	Not detected	-	Not detected
Dioxins / furans	0.10	0.00127	0.13	0.00093

3.1.1. Global Warming and GHG (Green House Gas) Emissions

Gaseous pollutants in the atmosphere are: Carbon monoxide (CO), carbon dioxide (CO₂), methane (CH₄), nitric oxide (NO), nitrogen dioxide (NO₂), nitrous oxide (N₂O), sulfur dioxide (SO₂), chlorofluorocarbons (CFCs) and ozone (O₃). CO₂ and CO are main greenhouse gases associated with global warming. At the present time, coal is responsible for 30–40% of world CO₂ emissions from fossil fuels. Global warming has been increasingly associated with the contribution of CO₂ (Figure 3) [28]. The use of bio-energy has the potential to greatly reduce our greenhouse gas emissions. Bio-energy generates about the same amount of carbon dioxide as fossil fuels, but every time a new plant grows, carbon dioxide is actually removed from the atmosphere. The net emission of carbon dioxide will be zero as long as plants continue to be replenished for bio-energy purposes.

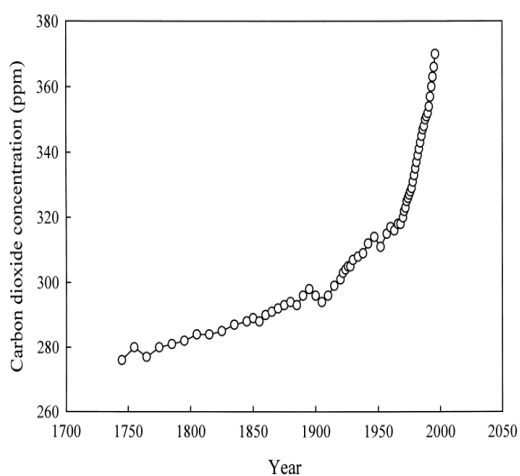


Fig. 3: Global carbon dioxide concentration rising in atmosphere [28]

It is estimated that CO₂ contributes about 50% to the anthropogenic greenhouse effect [28]. Earth surface temperature raising with the increases concentrations of CO₂, NO_x, CH₄, CFCs, Halons, Ozone, Peroxyacetylinitate throughout entrapped atmospheric heat [29]. Increased levels of greenhouse gases in the atmosphere are responsible for the warmer temperatures on the earth's surface. Temperature increases could destroy many fragile arctic ecosystems, as plants and animals cannot adapt quickly enough to keep pace with such a fast rate of warming. A global mean temperature rise of 1.5–4 K in the next century would have wide spread and complex impacts on the world's already strained ecosystems, many of which are very difficult to predict. Global warming could result in sea level raises, changes to patterns of precipitation, increased variability in the weather and a variety of other consequences.

The production and human use of energy contributes 60% of the human impact on global warming. Other activities which increase the level of greenhouse gases in the atmosphere are the use of chemicals such as chlorofluorocarbons (15%), agriculture (12%), land-use modifications (9%), and other human activities (4%). At the present time, the rate of world-wide greenhouse gas emissions is increasing every year. In order to prevent warming of more than a couple of degrees, atmospheric scientists feel that we must reduce our current level of emissions by about 60%. Minimizing the potential warming will require worldwide cooperation and quick action to improve energy efficiency, develop renewable sources of energy, stop the destruction of tropical forest and develop alternatives to chlorofluorocarbons (CFCs). The energy crops, such as fast-growing trees and grasses, are called bio-energy feed stocks. The use of bio-energy feed stocks can also help increase profits for the agricultural industry. The syngas produced is a renewable energy source that can provide additional greenhouse mitigation benefits through displacement of fossil energy sources. Thus the pyrolysis process is a technology that offers multiple benefits in greenhouse gas mitigation.

3.1.2. Mitigate acid rain

The term ‘Acid Rain’ is used to describe a rain or any other form of precipitation that is unusually acidic. It contains elevated levels of hydrogen ions (low p^H) as acidic deposition. Combustion of fossil fuels creates gaseous pollutants such as SO_2 and NO_x which are mainly contribute to acid rain. Highly acidic rain can damage or destroy aquatic life, forests, crops and buildings, as well as posing a threat to human health. Based on acidic deposition acid rain is describe in different ways: “wet” deposition such as rain, snow and fog and “dry” deposition in the form of acidic gases and dust. This acidity is a result of naturally occurring carbon dioxide (CO_2), which dissolves into water vapor in the atmosphere. Human activities such as the use of fossil fuels for energy can result in the release of sulfur dioxide (SO_2) and nitrous oxides (NO_x) in the atmosphere. In the atmosphere, SO_2 and NO_x react with water vapor to form weak solutions of nitric and sulfuric acid. Acid rain has a wide variety of environmental and health impacts. Acid rain can also result in human health concerns and damage to buildings. Acid rain can aggravate respiratory ailments such as bronchitis and asthma. Humans may also be affected by drinking water that contains higher levels of toxic metals that have been dissolved from soils and pipes by the increased acidity of drinking water supplies.

3.1.3. Soil amendments

Bio-char is known as "char" and "agri-char" which is produced from non-volatile components of biomass pyrolysis process. It is a stable form of carbon, highly resistant to decomposition due to its chemical structure and physical protection by interactions with clays. Bio-char has vital advantages with respect to soil ecosystem functions since it is more efficient in improving soil fertility and nutrient preservation than un-charred organic biomass matter [30-31]. Figure 4 shows that non bio-char material releases of all C after 100 years and it can be estimated to be less than 10–20% C remaining in agricultural soil after 5–10 years (depending on C quality and environment) [32]. However charring approximately 50% of the C contained in the biomass is immediately released and leaving a stable bio-char residue for long time (Fig. 4). The greater stable charcoal is produced at 400^0C to 1000^0C against oxidation by ozone, despite the fact that aromaticity of bio-char significantly increases above the temperature of 700^0C [33-34].

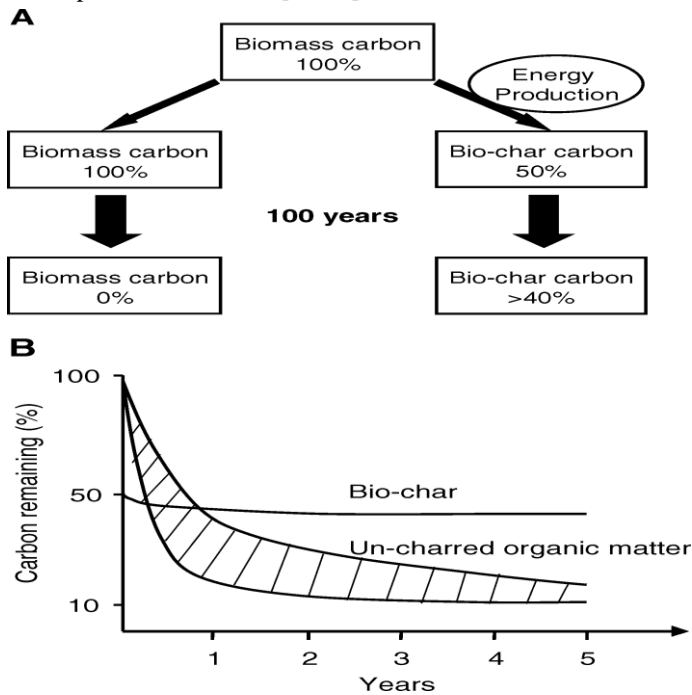


Fig. 4: (A) Carbon remaining from biomass decomposition and charring or pyrolysis carbon decomposition after 100 years [32], (B) range of biomass Carbon is remaining after decomposition of crop residues [35].

Bio-char applications to soil have the potential to decrease environmental pollution and have the ability to reduce CO_2 from atmosphere and emissions of other greenhouse gases. Virtually complete control of methane emissions at bio-char additions of 20 gkg^{-1} soil, N_2O emissions were reduced by up to 50% when bio-char was applied to soybean and by 80% in grass stands [36]. Bio-chars similar to black carbon in soil efficiently adsorbs ammonia (NH_3) and acts as a buffer for ammonia in soil, therefore bio-char helps to decrease ammonia volatilization from agricultural fields [37]. Lehmann, [32]

indicated that bio-chars works in soil as a very efficient adsorbent for dissolved ammonium, nitrate [38], phosphate [39], and other ionic solutes [40] as well as hydrophobic organic pollutants [41–42].

Application of bio-char as a soil amendment can remove carbon from the atmosphere. Bio-char becomes a beneficial soil amendment in worldwide. ‘Terra Preta’ soils in Brazilian Amazon region contained up to 70 times more black carbon than the surrounding soils [43]. It indicates that char is highly effective in increasing plant productivity in that region. Due to its highly recalcitrant nature, bio-char amendment will provide long-term increases in soil carbon stocks. Bio-char provides further mitigation of greenhouse gas emissions through reduction in nitrous oxide emissions from soil. Furthermore, use of bio-char reduces fertilizer requirements, thus reduce indirect greenhouse gas emissions from fertilizer manufacture. Microbial subsoil activity and the carbon content of the soils are key drivers of healthy soils to the way to increase soil carbon effectively and significantly and to encourage healthy microbial activity has been the subject of much experimentation and enquiry in recent years.

4. Conclusions

Environmental impacts of green waste to energy conversion via pyrolysis process have been discussed in this paper. Pyrolysis technology has strong adaptability to green waste to produce liquid fuels with high bio-oil yields. It offers a convenient solution for municipal waste management systems. Environmental, economic and social benefits need to be included in any comparative assessment with fossil fuel alternatives for long term success of bio-energy or green waste to energy conversion project. Green waste or biomass has good potential to become a significant fuel for distributed energy systems and a possible source of ‘green’ hydrogen at both small and large scales [44]. It can be expected that green waste will continue to provide an increasing amount of consumer energy for heat, electricity and bio-fuels for transport in an ecologically sustainable manner in future and will also avoid any adverse environmental impacts. The social benefits resulting from greater application of green waste pyrolysis process will become widely accepted technology as reliable and safe sources of providing energy services. Rural communities will overcome their decline energy situation by generating local power by using their local feedstock in a safe and environment friendly approach. Bio-char production while producing energy from green waste pyrolysis process offers a potential way to participate in active long term carbon sequestration in soil.

References:

- [1] EIA. Annual Energy Outlook 2006. Energy Information Administration, Washington, DC, U.S. Department of Energy.
- [2] Demirbas A. Biomass Resource Facilities and Biomass Conversion Processing for Fuels and Chemicals. *Energy Conversion and Management* 2001; 42: 1357 - 1378.
- [3] Asadullah M, Rahman M, Ali M, Motin M, Sultan M, Alam M. Jute Stick Pyrolysis for Bio-oil Production in Fluidized Bed Reactor. *Bioresource Technology* 2008; 99: 44-50.
- [4] Goyal HB, Seal D & Saxena RC. Bio-fuels from Thermochemical Conversion of Renewable Resources: A Review. *Renewable and Sustainable Energy Reviews* 2008; 504–517.
- [5] Bridgwater AV. Biomass fast pyrolysis. *Thermal Science* 2004; 8 (2): 21-49.
- [6] Downie A. BEST Pyrolysis Technology: A Solution for the Greenhouse Challenge. BEST Energies, Australia. *ThermalNet Newsletter* 2007.
- [7] Demirbas A. Potential applications of renewable energy sources, biomass combustion problems in boiler power systems and combustion related environmental issues. *Progress in Energy and Combustion Science* 2005; 31: 171–192.
- [8] Mohan D, Charles U, Pittman Jr. & Philip HS. Pyrolysis of Wood/Biomass for Bio-oil: A Critical Review. *Energy & Fuels* 2006; 20:848-889.
- [9] Aho A, Kumar N, Eranen K, Salmi T, Hupa M, Murzin DY. Catalytic pyrolysis of woody biomass in a fluidized bed reactor: influence of the zeolite structure. *Fuel* 2008; 87: 2493–2501.
- [10] Karaosmanoglu F & Tetik E. Fuel properties of pyrolytic oil of the straw and stalk of rape plant. *Renew Energy* 1999; 16: 1090–3.
- [11] Putun E, Uzun BB, Putun AE. Fixed-bed catalytic pyrolysis of cotton-seed cake: effects of pyrolysis temperature, natural zeolite content and sweeping gas flow rate. *Bioresource Technology* 2006; 97:701–10.
- [12] Ramage J, Scurlock J, Biomass. In: Boyle G², editor. *Renewable energy-power for a sustainable future*. Oxford: Oxford University Press 1996.
- [13] Zhang O, Chang J, Wang T, Xu Y. Review of biomass pyrolysis oil properties and upgrading research. *Energy Conversion and Management* 2007; 48:87–92.
- [14] Tsai, WT, Lee, MK, Chang, YM. Fast pyrolysis of rice husk: product yields and compositions. *Bioresour Technol* 2007; 98: 22–8.
- [15] M'ollersten K, Yan J, Moreira R. Potential market niches for biomass energy with CO₂ capture and storage—Opportunities for energy supply with negative CO₂ emissions. *Biomass and Bioenergy*, 2003; 25: 273 – 285.
- [16] Demirbas A. Biomass resources for energy and chemical industry. *Energy Edu Sci Tech*. 2000; 5: 21–45.
- [17] Ashwath N & Rank A. Green waste – A Potential Growth Medium for Plants, and a Valuable Feed Stock for Bioenergy and Biochar Production’ (Reporter, 2009).
- [18] Environmental Protection Agency, Queensland Government 2002, ‘Fact Sheet - "Green Waste" to Charcoal & Energy. Retrieved October 2007, from www.epa.qld.gov.au/sustainable_industries

- [19] Chowdhury A & Rasul M. Sustainable solution to the green waste management by thermo-chemical conversion process. Energy Congress on Alternative Energy Application, Kuwait 2009.
- [20] McKendry P 2002. Energy production from biomass (part 2): conversion technologies. *Bioresource Technology*; 83: 47–54.
- [21] Frassoldati A, Migliavacca G, Crippa, T, Velata F, Faravelli T, Ranzi E. Detailed kinetic modeling of thermal degradation of biomasses', Technical report 2006.
- [22] Pei-dong Z, Guomei J & Gang W. Contribution to emission reduction of CO₂ and SO₂ by household biogas construction in rural China. *Renewable and Sustainable Energy Reviews* 2007; 1: 1903–1912.
- [23] Thornley P, Upham P, Huang Y, Rezvani S, Brammer, J and Rogers, J. Integrated assessment of bioelectricity technology options. *Energy Policy* 2009; 37: 890–903.
- [24] Rowell R. *The Chemistry of Solid Wood*, American Chemical Society: Washington, DC 1984.
- [25] Grønli MG, Varhegyi G, Blassi CD. Thermogravimetric analysis and devolatilization kinetics of wood. *Industrial & Engineering Chemistry Research* 2002; 41:4201 – 4208.
- [26] Demirbas A. Pyrolysis of ground beech wood in irregular heating rate conditions. *Journal Applied Pyrolysis* 2005; 73:39–43.
- [27] Balat, M. Use of biomass sources for energy in Turkey and a view to biomass potential. *Biomass and Bioenergy* 2004; 29: 32–41.
- [28] Demirbas A. Bioenergy, Global Warming, and Environmental Impacts . *Energy Sources* 2004, 26:225–236.
- [29] Dincer I. Environmental issues: I—Energy utilization. *Energy Sources* 2001; 23: 69–81.
- [30] Sombroek W, Nachtergaele O and Hebel A. Amounts, dynamics and sequestering of carbon in tropical and subtropical soils. *Ambio* 1993;22: 417–426.
- [31] Lehmann J and Rondon M. Bio-char soil management on highly-weathered soils in the humid tropics. *Biological Approaches to Sustainable Soil Systems* 2005, Boca Raton, CRC Press, in press.
- [32] Lehmann J, Gaunt J and Rondon M. Bio-char Sequestration in Terrestrial Ecosystems – A Review. *Mitigation and Adaptation Strategies for Global Change* 2006; 11: 403–427.
- [33] Kawamoto K, Ishimaru K and Imamura Y. Reactivity of wood charcoal with ozone. *Journal of Wood Science* 2005; 51: 66–72.
- [34] Nishimiya K, Hata T and Imamura Y. Analyses of chemical structure of wood charcoal by X-ray photoelectron spectroscopy. *Journal of Wood Science* 1998; 44: 56–61.
- [35] Jenkinson DS and Ayanaba A. Decomposition of carbon-14 labeled plant material under tropical conditions. *Soil Science Society of America Journal* 1977; 41: 912–915.
- [36] Rondon M, Ramirez J and Lehmann J. Charcoal additions reduce net emissions of greenhouse gases to the atmosphere', in *Proceedings of the 3rd USDA Symposium on Greenhouse Gases and Carbon Sequestration, Baltimore, USA, March 21–24 2005*; 208.
- [37] Oya A and Iu G. Deodorization performance of charcoal particles loaded with orthophosphoric acid against ammonia and trimethylamine. *Carbon* 40 2002; 1391–1399.
- [38] Mizuta K, Matsumoto T, Hatate Y, Nishihara K and Nakanishi T. Removal of nitrate nitrogen from drinking water using bamboo powder charcoal. *Bioresource Technology* 2004; 95:255–257.
- [39] Beaton J, Peterson H and Bauer N. Some aspects of phosphate adsorption by charcoal. *Soil Science Society of America Proceedings* 1960; 24: 340–346.
- [40] Radovic L, Moreno-Castilla, C and Rivera-Utrilla, J. Carbon materials as adsorbents in aqueous solutions L.R. Radovic (ed.), *Chemistry and Physics of Carbon*, 2001; 227–405.
- [41] Gustaffson O, Haghseta F, Chan C, Macfarlane J and Gschwend P. Quantification of the dilute sedimentary soot phase: Implications for the PAH speciation and bioavailability. *Environmental Science and Technology* 1997; 31: 203–209.
- [42] Accardi-Dey A & Gschwend PM. Assessing the combined roles of natural organic matter and black carbon as sorbents in sediments. *Environmental Science and Technology* 2002; 36: 21–29.
- [43] Glaser B, Haumaier L, Guggenberger G, Zech W. The 'Terra Preta' phenomenon: a model for sustainable agriculture in the humid tropics', Published online: © Springer-Verlag 2001.
- [44] Sims R. Bio-energy to Mitigate for Climate Change and Meet the Needs of Society. *The Economy and the environment*' Kluwer Academic Publishers 2003; 8: 349–370.